COMPUTER SIMULATION OF AN OPTICALLY PUMPED METHYL FLUORIDE LASER

By

HARVEY CHARLES SCHAU III

A DISSERTATION PRESENTED TO THE GRADUATE COUNCIL
OF THE UNIVERSITY OF FLORIDA
IN PARTIAL FULFILLMENT OF THE REQUIREMENTS FOR THE
DEGREE OF DOCTOR OF PHILOSOPHY

UNIVERSITY OF FLORIDA

1975

THIS WORK IS DEDICATED TO THE

SCIENTISTS AND CREW OF THE R.V. GULFSTREAM

ACKNOWLEDGEMENTS

The author would like to thank his graduate committee and his department chairman, Dr. Knox Millsaps, for helpful discussions during the past year. The author would like to give particular thanks to his advisor and friend Dr. Dennis R. Keefer for suggesting and discussing the problem. Special thanks go to Dr. Willis B. Person of the Department of Chemistry for his encouragement and interest in the problem.

The author wishes to thank his parents Mr. and Mrs. Harvey C. Schau for moral and financial support and Miss Judith Van Der Walt for her excellent typing of the manuscript.

Lastly the author wants to thank his wife Sharron for her understanding and endurance of his ravings about methyl fluoride lasers for the past year, and his friends Falmouth, Monroe, Pete, and Fred for their welcome diversions.

TABLE OF CONTENTS

	page
ACKNOWLEDGEMENTS	iii
ABSTRACT	v
CHAPTER	
I. INTRODUCTION	1
II. ENERGY TRANSFER IN MOLECULES	29
III. METHYL FLUORIDE	39
IV. MODEL	53
V. RESULTS	62
VI. CONCLUSION	97
APPENDIX A	99
APPENDIX B	101
APPENDIX C	104
BIBLIOGRAPHY	106
BIOGRAPHICAL SKETCH	110

Abstract of Dissertation Presented to the
Graduate Council of the University of Florida
in Partial Fulfillment of the Requirements
for the Degree of Doctor of Philosophy

COMPUTER SIMULATION OF AN OPTICALLY PUMPED METHYL FLUORIDE LASER

By

Harvey Charles Schau III

August, 1975

Chairman: Dennis R. Keefer
Major Department: Engineering Sciences

Employing a semi-classical model, numerical solutions were obtained for a ten level model of methyl fluoride. Laser emission from methyl fluoride at approximately 16 microns was found to be possible by optically pumping with a carbon-dioxide laser. The methyl fluoride laser was found to have gain of approximately .51% per cm. and energy storage of approximately 31 $mJL^{-1}torr^{-1}$.

CHAPTER I - INTRODUCTION

Laser (La'zər) n. [l(ight) a(mplification by) s(timulated) e (mission of) r(adiation)]; a device, containing a crystal, gas, or other suitable substance, in which atoms, when stimulated by focused light waves, amplify and concentrate these waves, then emit them in a narrow, very intense beam, optical maser.[1]

Thus Webster defines the laser. Webster's definition exemplifies the importance and rapid growth of this new light source. Prior to the summer of 1960 however the word laser had an entirely different meaning; "Laser; the juice of the laser tree , laserpitium latifolium, also called silphium, greatly esteemed by the ancients as an antispasmodic , deobstrucent and diuretic."[2] Although the word has an ancient heritage, today it brings to mind a much more modern meaning. The laser is an example of the same idea ocurring to different people in different parts of the world at about the same time. The first lasers were actually masers (microwave amplifiers) which were jointly developed in 1951 by C. H. Townes of Columbia University and 1952 by N. G. Basov and A. M. Prokhorov of the USSR. For their work on coherent microwave amplifiers Townes, Basov, and Prokhorov were jointly awarded the Nobel prize in Physics in 1964. Following the development of the

maser, A. L. Schawlow of Bell Telephone Laboratories and Townes outlined the theory of an optical maser in 1958. After publication of this theory, T. H. Maiman in 1960 was the first to obtain actual laser action in the visible spectrum. Maiman employed a crystal of ruby as a lasing medium. This was suprising since at that time scientists were working on primarily gas lasers, and felt that probability of success was highest for gaseous devices. Time has proven their premonitions correct since most high power laser development in recent years has been from gases. Solid state lasers have,however,been found to be sources of tunable radiation important to ultra-high resolution spectroscopy, and recently glass lasers have been used in controlled fusion studies. Outside of these two areas new high power laser applications are being developed primarily around gas lasers.

Prior to the late sixties the laser was largely a scientific toy. It was at that time that molecular gas lasers were developed. These lasers,particularly the CO_2, have exhibited several important qualities. First is their efficiency (30-40%). This is extremely high when compared with efficiencies of less than 1% for most conventional lasers. Second, and perhaps more important, is their ability to be scaled up to industrial size. This gave great impetus toward developing commercially available high power CO_2 systems. In recent years CO_2 lasers have been moving out of the scientific laboratory

and into industry and the production line.[3,4,5]

Continuous wave (CW) lasing at 10.6 microns from CO_2 was first reported by C. N. K. Patel in 1964.[6] Since that date the CO_2 laser has undergone rapid improvement.[7] Attention is called to the review of CO_2 laser development by Robinson.[8]

Laser action from CO_2 proceeds via population inversion of vibrational levels. In electric discharge systems nitrogen is excited by electron collisions, which in turn excites the 00^01 antisymmetric stretch mode (see figure 1) of CO_2. Lasing is achieved from this level to either the 10^00 symmetric stretch at 10.6 microns or the 02^00 second bending mode at 9.6 microns (figure 2).[9] In order to maintain a population inversion the lower (01^10) level must be depleted. Normally helium is added to collisionally depopulate this level. In addition to undergoing ir active vibrational energy transitions, CO_2 may change its rotational energy by one quantum. This leads to a vibration-rotation spectrum of many-frequency laser lines in each the 10.6 micron band (figure 3). Each term labeled by J represents a rotational angular momentum state of CO_2 and thus a splitting of energy levels.[10] The terms R(J) and P(J) represent a transition of $\Delta J = -1$ and $+1$ respectively, following ir selection rules for CO_2. Figure 4 illustrates the wavelength difference for P,Q, and R bands $(Q;\Delta J = 0)$. Notice that odd J terms are missing. This is due to nuclear spin statistics for zero nuclear spin molecules

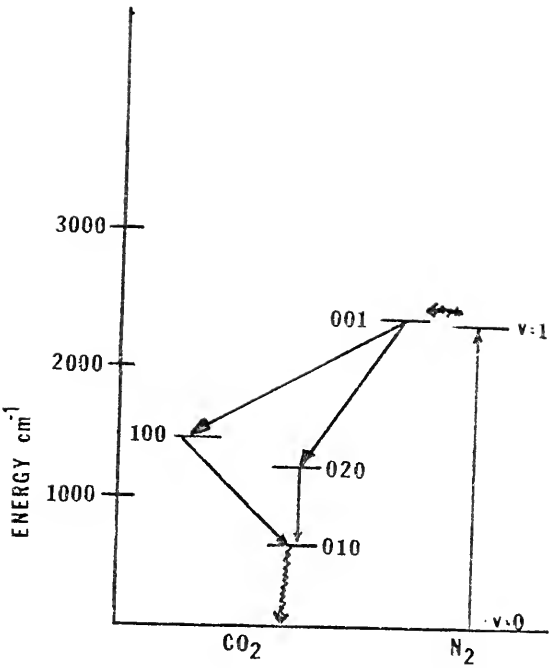

Figure 1. Energy levels of CO_2 and N_2 laser levels.

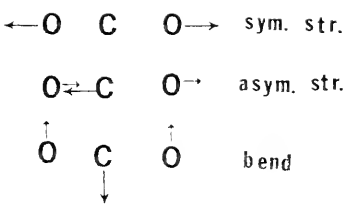

Figure 2. Laser vibrations of CO_2.

001-020 band CO_2

J	R(J)	P(J)
4	1067.50 cm^{-1}	1061.61
6	1068.89	1059.04
8	1070.43	1057.30
10	1071.87	1055.58
12	1073.28	1053.91
14	1074.63	1052.13
16	1076.00	1050.47
18	1077.30	1048.66
20	1078.57	1046.85
22	1079.85	1045.04
24	1081.08	1043.19
26	1082.29	1041.29
28	1083.48	1039.34
30	1084.63	1037.40
32	1085.74	1035.46
34	1086.84	1033.48
36	1087.90	1031.56
38	1088.97	1029.44
40	1090.04	1027.38
42	1090.99	1025.27
44	1092.00	1023.17
46	1093.01	1021.03
48	1093.85	1018.85
50	1094.81	1016.67
52	1095.71	1014.46
54		1012.25
56		1010.00
58		1007.76
60		1005.38

Figure 3. V-R spectrum of CO_2.

001-100 band CO_2

J	R(J)	P(J)
4	964.74	957.76
6	966.18	956.16
8	967.73	954.52
10	969.09	952.88
12	970.50	951.16
14	971.91	949.44
16	973.24	947.73
18	974.61	945.94
20	975.90	944.15
22	977.18	942.37
24	978.47	940.51
26	979.67	938.66
28	980.87	936.77
30	982.08	934.88
32	983.19	932.92
34	984.35	930.97
36	985.42	928.94
38	986.49	926.96
40	987.56	924.90
42	988.63	922.85
44	989.61	920.77
46	990.54	918.65
48	991.47	916.51
50	992.46	914.41
52	993.34	912.16
54	994.18	909.92
56		907.73

Figure 3. V-R spectrum of CO_2.

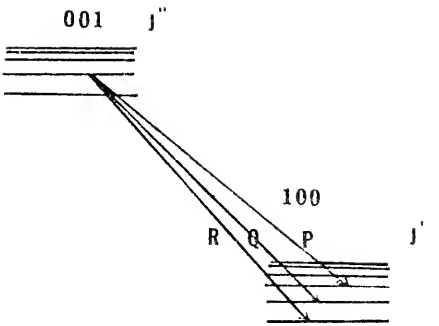

Figure 4. Diagram of V-R selection rules.

(for further discussion see Herzberg).

The theory of laser oscillation is easily understood if presented within the framework of amplifier dynamics. The laser as a device consists usually of a pair of parallel mirrors between which is placed the material which is to act as the amplifying medium over a limited frequency range (figure 5). L is the length of the active material and the optical distance will be denoted L'. If mirrors are placed on the ends of the cavity containing the amplifying material $L' = \eta L$ where η is the index of refraction. For gas lasers $\eta \simeq 1$ however the mirrors are usually located outside the laser cavity so that $L' > L$. At best one of the reflectors is partially transmitting so that its reflection coefficient (reflectivity) is less than one. The reflection coefficient r is defined as the fraction of light intensity reflected. Thus at each reflection, (1-r) of the intensity is transmitted as output. If the reflectivities of the two mirrors are r_1 and r_2 respectively, the energy of the wave is diminished by a factor $r_1 r_2$ in one transit. If the fraction of intensity remaining after one round trip through the laser is denoted by $e^{-2\gamma}$, γ is seen to be the loss coefficient per length. It is seen that

$$\gamma = -1/2 \text{ Log } r_1 r_2$$

if all other losses other than reflection are neglected. In gas lasers, diffraction losses are sometimes quite significant, but they will be neglected here.

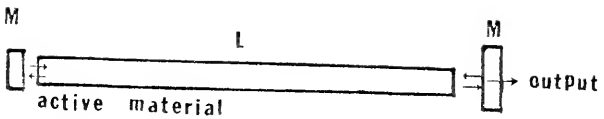

Figure 5. Diagram of gas laser.

Oscillation may be sustained if the amount of amplification per passage is equal to or greater than the losses. If the amplification per unit length is denoted by α_m, the threshold condition is seen to be

$$(1) \quad \alpha_m L = \gamma .$$

This equation also defines the amplification since the laser will always operate at threshold, as in electrical circuits. The amplification coefficient (negative of the absorption coefficient) may be written as

$$(2) \quad \alpha(\nu) = k(\nu)N$$

where ν = frequency

N = relative population difference between emitting and absorbing levels

$N = 1/N_0 (g_1/g_2 \ N_2 - N_1)$

g_1, g_2 are the quantum degeneracies of levels 1 and 2 respectively. N_1 and N_2 are the populations of levels 1 and 2 respectively. It can be shown that

$$(3) \quad k(\nu) = A_{21} / 8\pi\eta^2\nu^2 \ \ g_2/g_1 \ G(\nu\nu^0) = \kappa G(\nu\nu^0)$$

where A_{21} = Einstein spontaneous emmission coefficient (to be discussed later)

$A_{21}^{-1} = t_2$ the lifetime of atoms in level 2.

η = index of refraction

$G(\nu\nu^0)$ = lineshape around line center ν^0.

Combining equations (1), (2), and (3) we find

$$(4) \quad g_1/g_2 \ N_2 - N_1 = \gamma / L\kappa G(0)$$

where we assume emmision is at line center.

The time for a photon to make a single laser passage is $\tau = L'/C$ so that P_0 photons travelling through the laser after m passages will be reduced to

$$P = P_0 e^{-\gamma t/\tau}$$

thus the average photon lifetime may be defined as

$$(5) \qquad t_p = \tau/\gamma = L'/c\gamma.$$

Combining this with equation (4)

$$(6) \qquad \frac{g_1}{g_2} N_2 - N_1 = \frac{8\pi\eta^2\nu^2}{C^3 G(0)} \frac{g_1}{g_2} \frac{L'}{L} \frac{t_2}{t_p} \quad .$$

Equation (6) is known as the Schawlow-Townes condition, and gives the minimum population inversion necessary for lasing.

Once a population inversion has been established the principle of stimulated emission may be simply stated as: A photon will interact with a molecule in an excited state to produce two coherent photons travelling the same direction as the first, plus a molecule in the ground state. The initiation and maintenance of lasing action is most easily explained by use of the Einstein coefficients. These two coefficients are

spontaneous A_{12} [sec^{-1}] and

stimulated B_{12} [$cm^3 J^{-1}$ sec^{-2}].[9]

An excited state has probability P_{mn} of decaying from state m to state n defined as

$$P_{mn} = A_{mn} + U_\nu B_{mn}$$

where U_ν is the radiative density at the frequency satisfied by the Bohr condition. Note that A_{mn} and B_{mn} have

different units. A_{mn} is a measure of the natural lifetime of state m before spontaneous radiative decay to state n, analogous to noise in an electrical amplifier. Just as in the electrical analogy, the spontaneously emitted photons start the oscillations which lead to a radiation density thus stimulating more photons. Once the oscillations have reached threshold, the stiumlated term will continue to act as an amplifier as long as a population inversion is maintained. It is common in lasers for population inversion to be established and oscillation to start, where the rate of depletion of the upper level is faster than it can be refilled. In this case $g_1/g_2\ N_1 - N_2 < 0$ within a short time, and laser oscillations cease. This type of laser is called a pulsed laser, as opposed to a CW laser. CO_2 may be used as either and may be constructed in several different configurations. The earliest and simplest was by Patel (see figure 6).[11] It is interesting to note that the CO_2 was not placed directly in the discharge. Nitrogen is excited in the discharge and being homonuclear, is not ir active. CO_2 is then collisionally excited by the nitrogen to achieve a population inversion. Today commercial lasers place a 1-1-8 mixture of N_2- CO_2- He in the discharge to obtain pulsed or CW lasing.

An important advancement in CO_2 laser technology was the development of the TEA (Transverse Electric Atmospheric) laser.[12] As the acronym suggests this laser operates at atmospheric pressures thus eliminating the need for vacuum

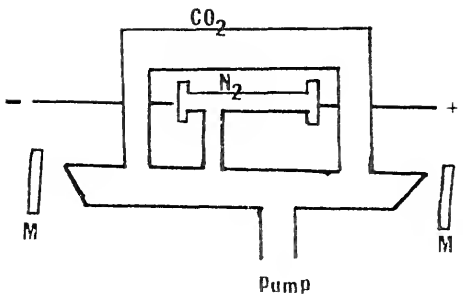

Figure 6. Early CO_2 laser by Patel.

systems and increasing power output. The pulse length is largely determined by the relaxation times of the gas molecules. As these become shorter at higher pressures, the pulse length decreases proportionally. Typical pulse length of a TEA laser is a few nanoseconds (1 nsec = 10^{-9}sec). It is difficult to achieve uniform excitation of CO_2 at atmospheric pressure, since at about 200 Torr the normal glow discharge constricts to an arc, heating the gas and destroying laser action. Several techniques have been developed to overcome this. Beaulieu originally used a very short 17 KV pulse to excite a transverse discharge between a row of pin cathodes and a round bar anode.[12] Today numerous TEA lasers use a helix geometry transverse discharge. The helix is designed to improve the uniformity of the discharge.

The radial radiation distribution in a cylindrical laser is very close to the eigenfunctions of a cylinder (see figure 7). Because of diffraction losses, the TEM_{00} mode propagates best, and to prevent mode switching and competition most lasers are operated by placing a stop within the optical cavity so that the laser operates in TEM_{00}.

It was indicated earlier that gas lasers radiate on many vibrational-rotational transitions. Because cavity quality factor is narrow compared with the Doppler or pressure broadened half width, the laser has longitudinal modes within the natural half width.[13] The condition for reinforcement is that $n\lambda=2L\eta$ or $\nu/c=n/2L\eta$, defining the optical distance

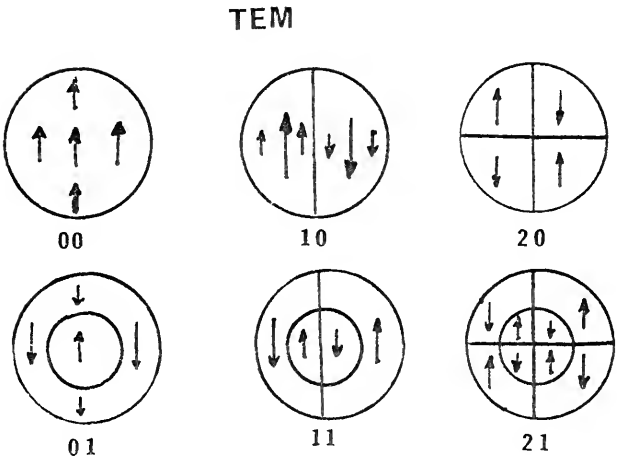

Figure 7.Radial distribution of radiation for cavity with circular mirrors. TEM (Transverse Electric and Magnetic) modes are indicated by arrows indicating magnitude of Electric field.

$$L' = \int_0^L \eta(z)\, dz$$

the condition for reinforcement becomes

$$\nu/c = n/2L'.$$

Thus the spacing between consecutive axial modes is

$$\nu_{n+1} - \nu_n = \Delta\nu = c/2L'.$$

Axial mode spacing is compared with natural line width in figure 8, notice that the cavity spacing is narrow with respect to the natural line. Only those cavity modes above threshold will lase, and in most gas lasers several axial modes will operate simultaneously giving multimode operation. There may possibly be from several to several thousand modes excited during laser operation.

It is of interest to consider the type of output that would result if a large number of modes, equidistant in frequency, could be excited with approximately equal amplitude, and, if these modes could somehow be locked together in a constant phase relationship. Each oscillating mode gives rise to a wave with an amplitude described by the real part of $e^{i\omega(t-x/c)}$ where $\omega = \omega_0 + k\Delta\omega$ and $\Delta\omega = 2\pi\Delta\nu$ ($\Delta\nu$ = half width of mode). The addition of $2n + 1$ of such waves with frequency centered around ω_0 all having equal amplitude leads to the expression

$$\sum_{k=-n}^{n} e^{i(\omega_0 + k\Delta\omega)t}$$

which is equal to $e^{i\omega_0 t}$ times the amplitude function $F(t) = \frac{\sin(n+\frac{1}{2})\Delta\omega t}{\sin \frac{1}{2}\Delta\omega t}$. The result of this synthesis is an amplitude-modulated wave of frequency ω_0, whose intensity

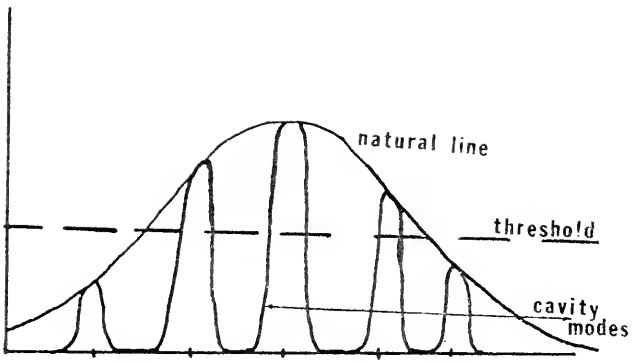

Figure 8.Axial mode spacing.

varies at the rate $F(t)^2$. Figure 9 illustrates a typical example. The peak intensity reaches $(2n+1)^2$ and the first zero of F(t) is separated from the peak by a time interval $\tau = T/2n+1$ where T is the period equal to $2\pi/\Delta\omega$. For a laser of optical length $L' = 60cm$, $T = 4x10^{-9}sec$. If 100 adjacent axial modes are locked together the resulting peak intensity is 10^4 times that of the individual modes, that is, 100 times the sum of all intensities. The peaks would repeat at the rate of $T^{-1} = 250MHz$ and peak pulses would have a half width of $4x10^{-11}$ sec.

Experimentally, phase-locking of the axial modes was first realized by means of an acoustic modulator incorporated in a He - Ne laser. Further experimentation with mode-locking revealed that it could be accomplished without the use of an externally driven modulator. Incorporation of a suitable bleachable absorber cell produces self-locking of the longitudinal modes. Figure 10 illustrates schematically the use of a bleachable absorbing cell as a mode locker. The complete description of this process requires a detailed mathematical analysis although several things can be said qualitatively.[14] The modes are all locked in phase when the dye cell is short and is located near one of the mirrors. Mode locking is accomplished by the nonlinear interaction of radiation of differing frequencies within the dye cell. The nonlinearity of the interaction is the consequence of the fact that the dye cell is operated in a region of intensity where the transitions are nearly saturated.

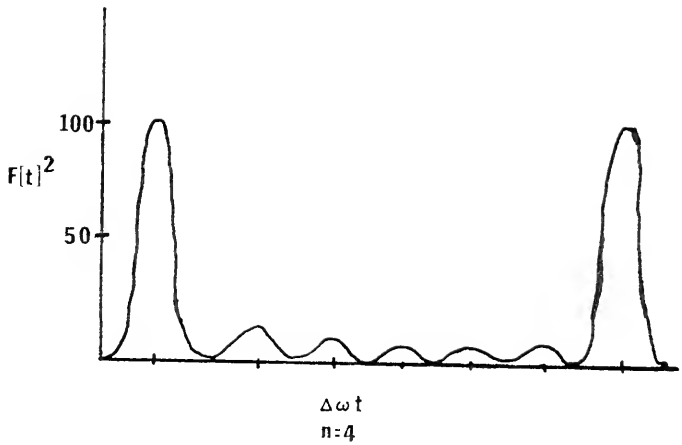

Figure 9. Example of mode locked pulses.

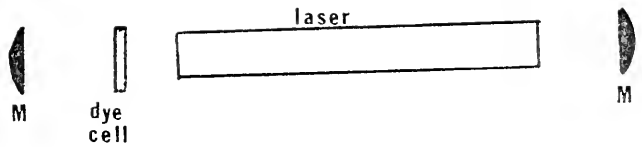

Figure 10. Mode locked laser.

The need for saturable absorbers was one of the early motivations for finding gases which efficiently absorbed laser radiation. In the case of CO_2, several gases were found such as SF_6, NH_3, PF_5, and CH_3F.[15] It was soon discovered however that laser absorption provided a means of preparing a molecule in an excited state in order to study energy transfer processes and chemical reactions. The criterion for good absorption of laser radiation is that the gas must have an energy level resonant with the laser emission. For infrared lasers, this corresponds to molecular vibrational frequencies, and it was soon discovered that the laser could play an important role in the study of a process mediated through vibrations such as chemical reaction.[16-23] Lasers have become an important tool in fluorescence studies, ultra high resolution spectroscopy, and molecular energy transfer, as well as developing passive mode lockers for other lasers.[24] Figure 11 shows a typical experimental set-up for a quasi- CW fluorescence experiment. Infrared fluorescence may be monitored from a gas which absorbs CO_2 radiation directly, or by the addition of a low concentration of sensitizer such as SF_6, the fluorescence from the collisionally excited molecule may be observed. Laser induced fluorescence spectroscopy is also a valuable technique for following the course of laser induced chemical reactions.[25,26] Molecules can be excited by the absorption of CO_2 laser radiation, and the kinetics of the subsequent reactions can be monitored by ir fluorescence spectroscopy.

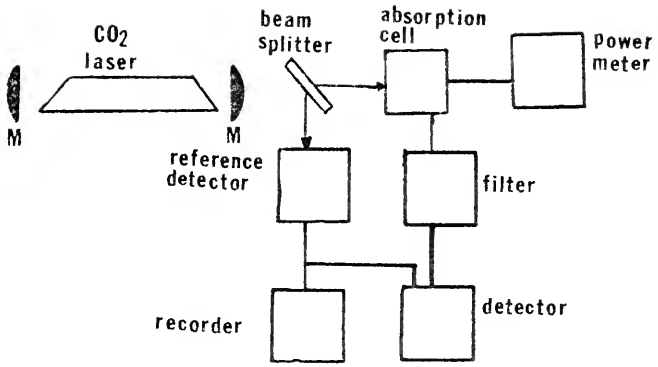

Figure 11. Experimental set-up of laser fluorescence study.

In general the reactions are monitored by observing the fluorescence from a given vibrational level as a function of time. Detailed energy transfer and evidence of non-Boltzmann chemical reactions have been observed in CH_3F, CH_3Cl, and CH_2Cl_2.[25,27]

If, as postulated, chemical processes can be affected by selectively exciting vibrational levels in one of the reactants producing non-equilibrium distributions, preferential reaction channels or increased reaction rates may be obtained. Possible applications of this technique include accelerated catalysis, efficient fractionation of hydrocarbons, and isotope separation. To date the possibility of stiumlating chemical reactions with lasers has been shown to be possible; however as yet there has been no large scale applications of non-Boltzmann chemical reactions.[28]

The possibility of separating isotopes with lasers has received much attention in recent years. The central idea is selective excitation of the isotopic species by a narrow band ir laser. This occurs because of the isotope shift, which is in the infrared portion of the spectrum, so that the laser leaves only a single isotope vibrationally excited. Photoionization may proceed from the excited molecule by a visible laser which would not contain enough energy to ionize the non-excited molecule. The ionized molecule may then be removed electrostatically or chemically.[23]

One major problem that must be overcome is the exchange of charge or vibrational energy between isotope and non-isotope before the separation takes place. This would mix the molecules enough so that no substantial increase in isotope concentration would result. Lasers may be the solution since a laser induced reaction might proceed rapidly.

Although the idea of laser isotope separation appears sound, in practice, few isotopes have been separated by either the photoionization, photon recoil, or induced chemical reaction method. One successful isotope separation has been with the isotope of clorine. The reason for this success is the fact that BCl_3 has an energy level resonant with CO_2 laser radiation. Not surprisingly,boron isotopes have also been separated by this process. There are however many isotopes which do not absorb resonantly with conventional lasers. It is the separation of these isotopes, which include uranium,that have stimulated interest in developing middle infrared lasers of high (several percent) efficiency.

The most important isotope separation problem today is the U^{235} - U^{238} pair for obvious reasons. A glance at the spectrum of UF_6 reveals that the absorption at 16 microns is by far more intense than other wavelengths and the isotope shift is largest there also.[29] A 16 micron gas laser does not currently exist and its

development has stimulated interest in several laboratories.

A new development that appears promising in generation of ir lasers is optical pumping with a conventional laser source. This eliminates the need for operation in an electric discharge or flowing gas chemical system which usually requires a homonuclear or metastable collision partner such as N_2 and H_2. The fundamental idea is absorption of laser radiation of one wavelength and regeneration at another. The quantum efficiency of such a process would be the ratio of the two wavelengths or about 62% for CO_2 absorption and 16 micron emission, although quantum efficiency is seldom approached. CO_2 lasers commonly operate with 20% efficiency which would yield a 16 micron laser with 1-2% efficiency. Although middle infrared lasers have not yet been generated in this manner, nearly 200 different wavelengths lasers in the far infrared have and it is hoped that this method will eventually provide lasers at nearly any desirable wavelength.[30-32] The application of optical pumping for generation of middle infrared lasers to be used in the study of isotope separation, laser induced chemistry, and ultra high resolution spectroscopy should deserve more and more attention in the future.

The author believes an important problem which may be solved by optical pumping is the development of a laser at approximately 16 microns for the separation

of uranium isotopes. By using a conventional laser source such as CO_2, a molecule may be excited and made to regenerate at around 16 microns. Figure 12 shows a diagramatic representation of the energy levels required for successful absorption of CO_2 radiation and regeneration at 16 microns.

The purpose of this paper is to demonstrate the feasibility of generation of middle infrared lasers by optical pumping. The particular wavelengths used will be absorption of CO_2 radiation and emission at 16 microns, although the ideas should be equally applicable to other needs.

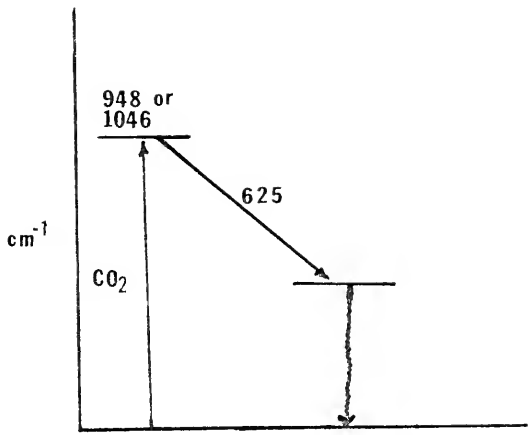

Figure 12. Expected energy levels leading to a 16micron laser.

CHAPTER II - ENERGY TRANSFER IN MOLECULES

Molecular energy transfer is important to both laser absorption and laser emission processes. For radiation in the infrared, energy transfer is largely in vibrational and rotational modes. Schrodinger's equation is written by assuming the Born-Oppenheimer approximation

(4) $\Psi(r,R) = \Psi_e(r)\chi_n(R)$

where $\Psi_e(r)$ is the electon wavefunction and χ_n is that for the nucleus. χ_n includes all nuclear terms such as vibrational and rotational motion. The energy is the sum of the individual contributions viz,

$E_{tot} = E_{trans} + E_{rot} + E_{vib} + E_{el} + E_{spin\text{-}orbit}$

Normally the contributions from infrared processes are those of vibrational and rotational motions. The electronic configuration is usually considered constant for infrared processes. Eigenfunctions for vibrational motion are usually found by first assuming a harmonic potential and adding anharmonic perturbations. The eigenfunctions for a harmonic potential are harmonic oscillator wavefunctions which lead to an evenly spaced spectrum with selection rules $\Delta v = \pm 1$ (see figure 13). The addition of anharmonic terms perturbs the spectrum

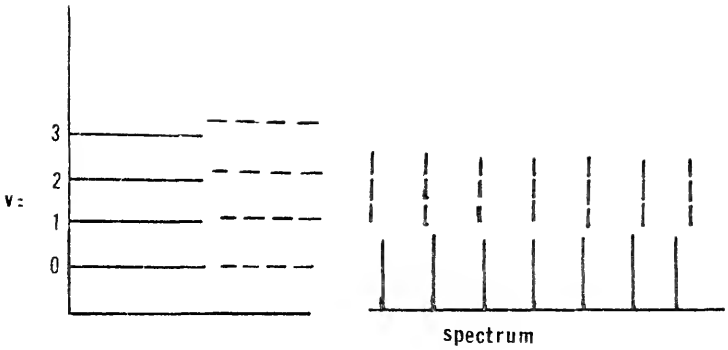

Figure 13. Spectrum of harmonic oscillator.

qualitatively as shown by the dashed lines.

As indicated earlier, rotational energy splits each vibrational energy level into many sublevels, the eigenfunctions of which are found by assuming a rigid rotor Hamiltonian and are proportional to spherical harmonic functions. This leads to selection rules $\Delta J = 0, \pm 1$, for a totally symmetric electronic wavefunction.[33] Figure 14 shows the energy levels of a rigid rotor and indicates dipole-allowed transitions.

Emission or absorption of light is usually explained within the framework of time dependent perturbation theory.[34] After separating the unperturbed Hamiltonian into vibrational, rotational, and electronic motion, solutions are found in the absence of any electromagnetic radiation. The oscillating field is then treated as a perturbation and first order quantities such as probabilities of transition from one stationary state to another, and energy corrections are calculated. If one writes the perturbing hamiltonian as

$$H'(Rt) = H'(R)e^{\pm i\omega t}$$

then the probability of the system being in state m at time t (after starting in state k) for a dipole transition is

$$(7) \qquad |C_m(t)|^2 = 4|H_{mk}|^2 \sin[(E_k - E_m \pm h\omega)t/2h]/(E_k - E_m \pm h\omega)^2$$

where E_m, E_k are the energies of the m and k states. The case where $E_m = E_k \pm h\omega$ is called resonance absorption or emission (depending on the sign), and for this case

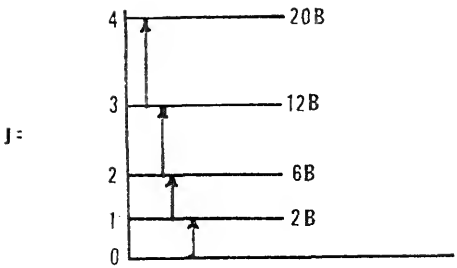

Figure 14. Energy levels of rigid rotor.

the transition probability depends linearly on time for short times. (Recall that this is only a perturbation approach and the interaction must still be small or occur for a short time.) The matrix elements coupling the states may be written

$H_{mk} = < m|H'(R)|k > = <\psi_m|H'(R)|\psi_k>$

where the wave functions are those calculated from the unperturbed Hamiltonian. A first order calculation results in

$$H_{mr} = \bar{E}\mu(mk)$$

where $\mu(mk)$ is the transition dipole moment

$$\mu(mk) = < m|\mu|k >$$

and μ is the permanent dipole of the molecule.

The probability of a level changing from state k to m in a radiation field with a finite spectrum rather than simply a monochromatic field may be found by integrating (7) over the frequency domain and averaging over all spatial directions. The result may be written in terms of the Einstein stimulated emission coefficient

$$P_{k\to m} = U_\nu B_{mk}$$

where U_ν is the radiation density at frequency corresponding to energy difference of levels m and k, and B_{mk} is the Einstein stimulated emission coefficient

$$B_{km} = 8\pi^2/3h^2|\mu(mk)|^2$$

Transitions which are forbidden; those for which the transition dipole (or dipole moment) are identically zero are found by symmmetry operations and it is usually

relatively easy to find which states are not infrared active.[33]

The mechanism by which laser action initiates and subsequently amplifies is most easily explained with use of the Einstein coefficients. In the early part of this century it was shown by A. Einstein that a resonant photon travelling in one direction could react with an excited molecule and produce two coherent photons traveling in phase, plus an unexcited molecule. Once laser action is started, the laser medium acts like an amplifier. The probability of an excited system undergoing such a transition in a radiation field of energy density U_ν has already been given as

$$P_{2\to1} = U_\nu B_{12}$$

and similarly for absorption. This does not, however, explain how any radiation gets started in the cavity since initially for zero radiation there is zero probability of initiation. Actually, atoms or molecules in excited states remain so only for limited periods of time due to the Heisenberg uncertainty principle. The uncertainty may be expressed

$$\Delta E\ \Delta t \simeq h \qquad \text{or}$$

$$\Delta\nu\ \Delta t \simeq 1$$

so that for an ensemble of molecules of lineshape with half width $\Delta\nu$ the excited state can be expected to decay spontaneously within Δt. Therefore we must add a term to our probability for a molecule to go from state 2 to

state 1: $P_{2\to1} = U_\nu B_{21} + A_{21}$.

A_{21} is the Einstein spontaneous emission coefficient (Δt^{-1}). Thus we see that it is through the natural decay that noise is able to start the laser amplifier.

Vibrational or rotational energy can be transferred collisionally as well as through radiative transition (for infrared we do not consider electronic transitions). Collisional transitions occur when one molecule collides with a second and transfers some, or all, of its energy to the different degrees of freedom of the second molecule. This energy may go into rotational, vibrational, or translational energy of the second molecule. The time a molecule remains in an excited state before the energy redistributes back to equilibrium conditions is called the relaxation time. In optical pumping, energy transfer can proceed three ways; transfer from one excited vibrational state to another (V-V), transfer from an excited vibrational state to higher rotational energy (V-R), and transfer from an excited vibrational state to the translational motion of the molecule as a whole (V-T). It is commonly believed that $\tau_{v-v} < \tau_{v-R} < \tau_{v-T}$ where τ is the relaxation time for that particular process and we assume that transfer within one vibrational mode is faster than between two different modes.[20,23,35]

Theoretical accounts of collision processes have only moderate success in predicting probability of energy transfer. The reader is referred to an excellent review

of the theoretical treatment of collisional energy transfer by Bailey and Cruickshank.[36] The most popular theory to compare with experimental results is a quantum mechanical V-T theory developed by Schwartz, Slawsky, and Herzfeld (SSH theory).[37] SSH theory, as well as most others, does not succeed in providing absolute probabilities. However it does predict that resonant processes (those for which the second of the colliding pair has an energy level resonant with the excited level of the first) have the largest relative probability,and that pairs with a smaller reduced mass will have higher probability of energy transfer than others.

Although there are no rigorous selection rules for molecular collisions, there appear to be some collisional transfer processes which occur with much higher probability than others. This is based on the fact that symmetric states do not combine with antisymmetric for any kinds of transitions including collisions. It is for this reason that the two modifications of symmetric top molecules such as NH_3, CH_3Cl, CH_3F (e,a) are transferred into each other only extremely slowly, just as are ortho- and para- hydrogen.[38]

Recently Oka has given some approximate selection rules observed by microwave studies of NH_3 and the qualitative interpretation of them.[39] To summarize these he finds

(i) Collision-induced transitions with dipole selection rules ($\Delta J = 0, \pm 1$, parity $+ \leftrightarrow -$) are "preferred".

(ii) The $\Delta J = 0$ dipole-type transitions (same selection rules as dipole transitions) have much greater probability than the $\Delta J = \pm 1$ dipole-type transitions for levels with $J \simeq K$ but they have probabilities of equal order of magnitude for levels with $J >> K$.

(iii) The $\Delta J > 1$ transitions have much smaller probabilities than the $\Delta J = \pm 1$ transitions.

(iv) The $\Delta K \neq 0$ transitions have much smaller probabilities than the $\Delta K = 0$ transitions.

(v) It is suggested that $\Delta J = \pm 1$ quadrupole-type transitions (parity $+ \leftrightarrow +$) are the same order of magnitude as those of the corresponding dipole transitions.

These "selection" rules are very important since most experiments measure the rate of transfer of vibrational energy between different modes of a molecule or different molecules, although they don't give information as to the particular rotational levels involved.

We have seen in this chapter that there are two basic energy transfer mechanisms: radiative and collisional. Both are important to lasers, sometimes beneficial sometimes detrimental. Radiative transitions are obviously most important when optically pumping a gas with a laser such as CO_2; however if laser action is expected from any level other than that pumped, one must rely on collisions to transfer energy selectively into that level.

Transitions due to the natural lifetimes of the state must initiate stimulated emission before collisions populate the lower state, thus depleting the population inversion. Both spontaneous and stimulated coefficients must be known as well as the collisional rates and their selection rules if one is to successfully predict how a collection of molecules will react after optical pumping. The regeneration of laser radiation at a different frequency will be a function of all three processes.

CHAPTER III - METHYL FLUORIDE

The success of producing an optically pumped laser is largely dependent on the gas to be used as a lasing medium. It must absorb CO_2 laser radiation strongly and be able to achieve a population inversion between two levels that would result in 16 micron emission. When modeling a process such as this, a good deal of information is required to accurately predict the results.

The first area that must be understood is the absorption process. It must be known how strongly and on what CO_2 line the gas absorbs. A high resolution spectrum is helpful to see to what degree the gas and pumping lineshapes overlap. Normally, one is not given this information, rather an experimental absorption coefficient is given for a particular CO_2 line. The overlap integral may still be estimated if the Einstein coefficients can be found from vibrational band intensity measurements which have been carried out for many molecules. In general the absorption coefficient will depend on the particular rotational levels involved, line broadening, degree of resonance, and pressure. One advantage of modeling a process such as this is that these parameters may be changed and the absorption coefficient still known

if a measurement has been carried out for any one particular set of parameters.

The second area of importance is the collision kinetics of the molecule. This is important to the problem of rotational bottlenecking. Often during laser operation, a particular rotational state will be filled faster than the collisional rotational relation can relax it. When this occurs, the population inversion cannot be maintained and lasing stops. The bottleneck effect is so termed because it is normally the process that limits laser efficiency. Within this area also,is the V-V energy transfer process. If laser action is expected from any level other than the upper state of the pumping process, energy will have to be transferred via V-V collisions. The time scale and efficiency of these collisions will be very important to the success of the laser.

The gas to be used in generation of a 16 micron laser by optically pumping with CO_2 must strongly absorb CO_2 radiation, and must have two levels separated by approximately 624 cm^{-1}. The lower level must be far enough above ground, that there is no appreciable thermal population. Although several molecules fulfill the above requirements, only one has had enough experimental work done on it to make it attractive. The molecule, methyl fluoride (CH_3F),had been used as a saturable absorber in CO_2 mode-locking studies and far infrared

laser generation,[30-32] a source of photon echoes in phase coherence studies,[40] and recently the collisional kinetics have been studied by following laser induced fluoresence.[25]

Figure 15 displays the energy level diagram for methyl fluoride. The ground state to $V_3 = 1$ transition is at approximately 9.55 microns which is within the 9.6 band of CO_2.[41] The second excited state of V_3 is reported at 2081 cm^{-1} and the lower pair of the V_{25} doublet hybrid band is reported approximately at 1460 cm^{-1}.[42]

Methyl fluoride is a symmetric top molecule with C_{3v} symmetry.[38] The rigid rotor term values are given by

$$F(J,K) = AJ(J+1)+(A-B)K^2$$

where J is the total angular momentum and K is the component of J on the internuclear axis. The constants A and B are defined as

$$A = h^2/2cI_a \ , \quad B = h^2/2cI_b$$

where I is the moment of inertia about that particular axis. Selection rules yield radiative transitions (rigid rotor, harmonic oscillator) $\Delta J=0,\pm1,\Delta K=0,\pm1$ which lead to the following term symbols, labeled

$$^{K}J(J_{lower},K_{lower})$$

$$^{Q}Q(J,K)=\nu_0$$

$$^{Q}P(J,K)=\nu_0+2AJ$$

$$^{Q}R(J,K)=\nu_0-2A(J+1)$$

$$^{P}Q(J,K)=\nu_0-(A-B)(2K+1)$$

$$^{P}P(J,K)=\nu_0+2AJ-(A-B)(2K+1)$$

$$^{P}R(J,K)=\nu_0-2A(J+1)-(A-B)(2K+1)$$

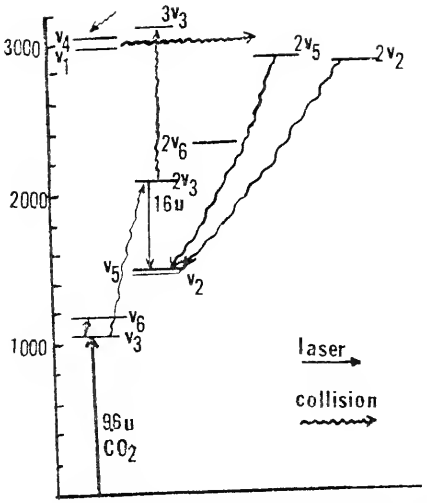

Figure 15. Energy levels of CH_3F.

$$R_Q(J,K)=\nu_0+(A-B)(2K+1)$$

$$R_P(J,K)=\nu_0+2AJ+(A-B)(2K+1)$$

$$R_R(J,K)=\nu_0-2A(J+1)+(A-B)(2K+1)$$

Actually the rotational constants change slightly from one vibrational level to the next and centrifugal distortion terms may be included so that the spectrum is slightly more complicated than is indicated here.

Thus it may be seen that the spectrum of methyl fluoride is quite complex. Parallel bands, those for which the dipole changes parallel to the applied field have selection rules $\Delta K=0$, while perpendicular bands have $\Delta K=\pm 1$. It is customary to make the following vibrational assignments for methyl fluoride.[43] Actually the V_2 and V_5 vibrations must be considered degenerate thus creating a V_{25} and V_{52} hybrid pair. This band is composed of both a perpendicular and a parallel band. The transition from $V_3=2$ to V_{25} to be considered should therefore have several rotational lines on which lasing could occur around 16 microns.

Vibration	Frequency(cm^{-1})	Species	Type
V_1- CH_3 s-stretch	2930	a	parallel
V_2- CH_3 s-deform	1464	e	parallel
V_3- CF stretch	1049	e	parallel
V_4- CH_3 d-stretch	3006	e	perpendicular
V_5- CH_3 d-deform	1467	e	perpendicular
V_6- CH_3 rock	1182	e	perpendicular

Methyl fluoride has been used as an absorber of 9.6 micron CO_2 radiation and absorption on the P(20) and P(32) CO_2 lines has been reported. The P(20) absorption is believed to be the $^{Q}Q(12,1)$ and $^{Q}Q(12,2)$ meythl fluoride transition while the P(32) absorption is due to another isotopic species of methyl fluoride.[30-32] The lack of absorption of other CO_2 wavelength is somewhat suprising since a medium resolution spectrum exhibits a large Q branch centered around the P(18), 9.6 CO_2 band.[44] Closer inspection reveals the K splitting of this branch may account for the possibility that the extremely narrow laser line can fit between two methyl fluoride transitions. The laser used for this experiment was a Q-switched mode-stabilize CO_2 and the possibility of hole burning exists. The effect of a TEA laser pulse or a mode stabilized TEA laser can be modeled as described in Chapter I. This can be written into any simulation scheme and results checked to observe the effect of different forms of pumping radiation.

Recently the collisional kinetics and energy transfer have been studied by monitoring fluorescence rise times from various levels after pumping the V_3=1 with a CO_2 laser.[25, 35, 45-48] This technique has been fruitful in observing collisional energy transfer from a particular vibrational level to a diluent gas also.[49] Figure 16 indicates the relative speed of V-V transfer after pumping the V_3=1 level in methyl fluoride. The results

(1) Excitation of V_3 by 9.6 P(20) CO_2

(2) $2CH_3F(V_3) \rightleftharpoons CH_3F10) + CH_3F(2V_3) + 10\ cm^{-1}$

$CH_3F(2V_3) + CH_3F(V_3) \rightleftharpoons CH_3F(0) + CH_3F(3V_3) + 20\ cm^{-1}$

10 collisions

(3) $CH_3F(3V_3) + CH_3F(0) \rightleftharpoons CH_3F(0) + CH_3F(V_1) + 120\ cm^{-1}$

$CH_3F(3V_3) + CH_3F(0) \rightleftharpoons CH_3F(0) + CH_3F(V_4) + 100\ cm^{-1}$

70 collisions

(4) $CH_3F(V_1) + CH_3F(0) \rightleftharpoons CH_3F(0) + CH_3F(2V_2)$

$CH_3F(V_1) + CH_3F(0) \rightleftharpoons CH_3F(0) + CH_3F(2V_5)$

$CH_3F(V_4) + CH_3F(0) \rightleftharpoons CH_3F(0) + CH_3F(2V_2)$

$CH_3F(V_4) + CH_3F(0) \rightleftharpoons CH_3F(0) + CH_3F(2V_5)$

10 collisions

(5) $CH_3F(2V_2) + CH_3F(0) \rightleftharpoons 2CH_3F(V_2) - 10\ cm^{-1}$

$CH_3F(2V_5) + CH_3F(0) \rightleftharpoons 2CH_3F(V_5) - 10\ cm^{-1}$

50 collisions

(6) $CH_3F(V_3) + CH_3F(0) \rightleftharpoons CH_3F(0) + CH_3F(V) - 133\ cm^{-1}$

40 collisions

(7) $CH_3F(V\text{-}T/R)$ 15,000 collisions

Figure 16. V-V,V-T/R rates for methyl fluoride.

were obtained by monitoring the fluoresence risetime in an experiment similar to one described in Chapter I. The processes are step-wise in that they follow in the order indicated. Comparison with SSH breathing sphere amplitudes reveal the relative collision rates are in good agreement although as is usually true, absolute probabilities are not.[46, 47]

The very long V-T time is due to the fact that the lowest level of methyl fluoride is still over 1000 cm^{-1} above ground. By using a double resonance experimental setup, where a particular rotational level is populated into the upper vibrational state, and microwave absorption monitored as a function of time for $\Delta J=1$, $\Delta K=0$ in $C^{13}H_3F$ the rotational relaxation was found to be $T = (10.5\pm6)\,\mu sec/mtorr$. which is long as compared with the V-V rates.[50]

As can be seen from the preceding discussion, a great deal is known about methyl fluoride. Figure 17 indicates the match up between known CO_2 laser lines and the theoretical methyl fluoride spectrum around the reported P(20) absorption.[44, 51] Other CO_2 lines have close coincidence, although we will primarily discuss the P(20). This figure clearly indicates that even high resolution is not enough to guarantee good absorption of CO_2. Due to the number and narrowness of methyl fluoride absorption lines, one might expect little absorption of a CO_2 line that chanced to fall between two methyl

J	K	q_Q term value	
12	0	1046.837	Reported CO_2 line 1046.85
12	1	1046.827	P(20) absorption
12	2	1046.826	reported.
12	3	1046.824	
12	4	1046.821	
12	5	1046.817	
12	6	1046.813	
12	7	1046.808	
12	8	1046.802	
12	9	1046.796	
12	10	1046.788	
12	11	1046.780	
12	12	1046.771	

Half width CH_3F; $2.21 \times 10^{-3} cm^{-1}$ at 1 torr.
Half width CO_2; $2\text{-}32 \times 10^{-3} cm^{-1}$ at 1-40 torr.
Cavity width CO_2; $10^{-5} cm^{-1}$.

Figure 17. Theoretical spectrum of CH_3F

fluoride lines. The question of how pressure broadening of both CO_2 and methyl fluoride affects absorption has not been answered. It is probably true that the $^{Q}Q(12)$ transition is involved instead of the next closest $^{Q}P(1)$ since the thermal population peak is around J = 11.[31, 32] Lasers which operate on a single axial mode, tunable over their doppler width have recently been made commercially available and will no doubt play an important role in studying and maximizing absorption in molecules such as methyl fluoride.

Of course the real interest of this study is the generation of a 16 micron laser. Figure 18 shows the approximate expected spectrum for V_3= 2 to V_{25} transition. The rotational constants are not accurately known for either level so the ground state to V_3=1 rotational constants were used.[32, 43] These may be in error by several wave numbers; however it serves to give an idea of the relative differences among transitions.

Although this paper is concerned with the computer simulation of laser construction, Figure 19 illustrates a typical laboratory construction of an optically pumped laser. The KB_r prism acts as a dispersing element thus enabling reflection of the CO_2 and 16 micron radiation to physically take place in different regions. The grating is needed to operate on the 9.6 band since gain is normally higher in the 10.6 region. Mirrors M_1 and M_2 should be gold or dielectric coated to reflect at 16 microns.

	J'=12, K'=2			J'=12, K'=1		
	F(J,K)	J"	K"	F(J,K)	J"	K"
q_Q	619.23	12	2	619.23	12	1
q_R	641.07	11	2	599.07	13	1
q_P	599.07	13	2	641.07	11	1
r_Q	631.57	12	2	622.78	12	0
p_Q	596.37	12	3	605.17	12	2
r_R	651.73	11	1	642.93	11	0
p_R	616.52	11	3	625.32	11	2
r_P	607.73	13	1	600.93	13	0
p_P	674.53	13	3	583.33	13	2

Figure 18. $2V_3$-V_{25} approximate spectrum.

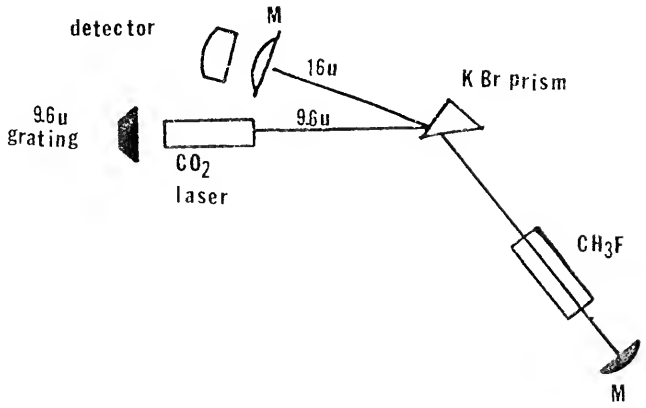

Figure 19. Construction of methyl fluoride laser.

If a line other than that at 16 microns has a lower threshold, it will lase first. In this event, mirror M_2 will have to be replaced with a grating so that the cavity becomes tuned to 16 microns.

It can be seen in figure 19 that there are many different external conditions under which lasing may be attempted. These include gain length, pressure, mirror reflectivities, pump power and duration, and type of CO_2 pumping. The purpose of this simulation is to check the effect of different parameters and narrow the conditions under which one should expect laser action. This will eliminate much trial and error experimental work and should help in the planning and construction of the laser.

A second area where computer simulation is expedient is the determination of how accurately a particular molecular constant is needed to be known for accurate prediction of laser generation. This will help plan additional experiments which need to be performed prior to laser construction. In the case of methyl fluoride there are two areas of importance that may need further study. The first is the absolute frequency of the $V_3 = 2$ to V_{25} transition. This will have to be measured if it is deemed important. The second area of importance is the life-time of the $V_3 = 2$ state in methyl fluoride. This is important because a long lifetime (determined by the Einstein spontaneous emission coefficient) will allow the level to collisionally populate, thus depleting the

population inversion. The spontaneous emission acts as an initiator of laser action and must initiate rapidly enough to allow the energy to transfer radiatively from $V_3 = 2$ to $V_{25} = 1$ rather than collisionally. Thus the competition between collisional and radiative lifetimes may be extremely important. An important aspect of modeling as we have described, is that the collision rates are known. This should enable us to predict for what range of values of the Einstein coefficient to expect lasing. It is conceivable that a rough estimate within a factor of 100 is all that is needed to assure lasing, or an accurate measurement may have to be made if the results are very sensitive to the actual numerical value. We believe that the Einstein coefficient for the $V_3 = 2$ state may be estimated fairly accurately from the Einstein coefficients for the $V_3 = 1$ level. This coefficient may be determined by intergrated intensity measurements using the relation

$$\Gamma(\text{cm}^2\ \text{mole}^{-1}) = 2.505 \times 10^2 B_{12}^I$$

substituting the measured value for Γ yields.[52]

$$\Gamma = 9055.6 \pm 10\%$$

$$B_{12}^I = 6.8 \times 10^{23}\ \text{cm}^3\ \text{J}^{-1}\ \text{sec}^{-2}$$

It is expected that the Einstein coefficient for the $V_3 = 2$ to $V_{25} = 1$ will be substantially smaller than B_{12} since the transition is forbidden by harmonic oscillator selection rules ($\Delta V \neq 2$). Thus by estimating the coefficient for this transition we may determine roughly to what accuracy it must be known. See Appendix B.

CHAPTER IV MODEL

The model which we employ is a standard kinetic rate equation used by many authors. The two types of terms are those for radiative[52] and collisional[35] transitions. Figure 20 shows the interaction of different levels in this model. This figure should be compared with the energy level diagram for methyl fluoride in figure 14. We assume that collisionally $\Delta K = 0$, $\Delta J = 0$ selection rules predominate so that relatively few rotation levels need to be represented. The V_{25} state is represented by two rotational levels, one for collisional population and one for radiative population since it is desired to see what effect the different symmetry combinations have on lasing. Rotational levels of methyl fluoride are of two types, the K = 0,3,6,...are symmetric (type a) while the K = 1,2,4,5,...levels are asymmetric (type e). Levels with overall species e are doubly degenerate, thus direct product tables show that the V_1 level has rotational levels a and e, while the others have only the a rotational level; these yield the overall e state (a x e = e) while the e rotational level gives an a + a + e(e x e = a + a + e).[38] Molecules of methyl

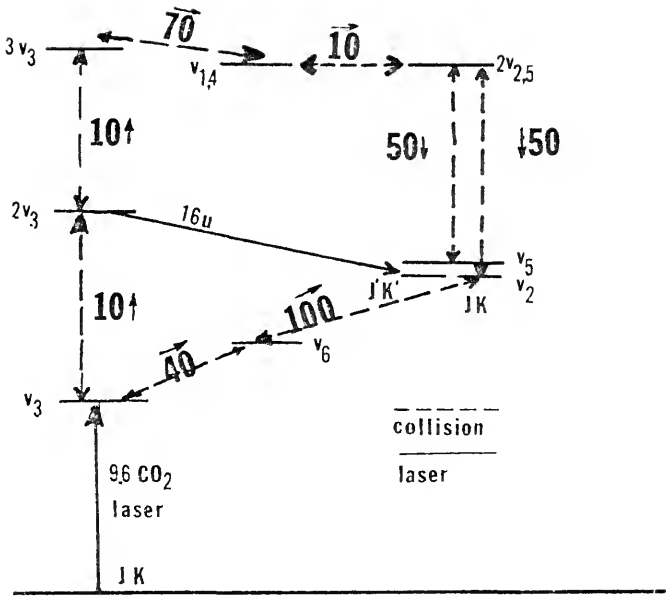

Figure 20. Schematic representation of model. (large numbers indicate number of collisions and arrows, the direction for that rate.)

fluoride in the ground state are either in rotational type a or e so that even collisionally, little mixing is expected. The possibility of changing rotational levels by $\Delta K = 0, \pm 1$ exists, since V_2 is actually a hybrid (parallel and perpendicular allowed transitions) and thus the lower laser level could possibly be a different symmetry than the upper level which is filled collisionally. The equations when non dimensionalized in time with respect to collision frequency, number density with respect to density of the ground rotational level, and laser output with respect to the input CO_2 power assume the form

$$\frac{d\Psi}{dt} = Q\Psi\left(N_{2V3} - \frac{g_{2V3}}{g_{V25}} N^L_{V25}\right) + P\Psi$$

$$\frac{dN_{V3}}{dt} = r_2\left(N_0 N_{2V3} - e^{10/kT} N^2_{V3}\right) + r_4\left(N_0 N_{3V3} - e^{20/kT} N_{2V3} N_{V3}\right)$$

$$+ r_{12}\left(N_0 N_{V6} - e^{133/kT} N_0 N_{V3}\right) + Z_{11}\Phi\left(N_0 - N_{V3}\right)$$

$$\frac{dN_{2V3}}{dt} = r_2\left(e^{10/kT} N^2_{V3} - N_0 N_{2V3}\right) + r_4\left(N_0 N_{3V3} - e^{20/kT} N_{2V3} N_{V3}\right)$$

$$- Z_{23}\Psi\left(N_{2V3} - \frac{g_{2V3}}{g_{V25}} N^L_{V25}\right)$$

$$\frac{dN_{3V3}}{dt} = r_4\left(e^{20/kT} N_{2V3} N_{V3} - N_0 N_{3V3}\right) + r_5\left(N_0 N_{V41} - e^{110/kT} N_0 N_{3V3}\right)$$

$$\frac{dN_{V41}}{dt} = r_5\left(e^{110/kT} N_0 N_{3V3} - N_0 N_{V41}\right) + r_6\left(N_0 N_{2V25} - N_0 N_{V41}\right)$$

$$\frac{dN_{2v25}}{dt} = r_6(N_0 N_{v41} - N_0 N_{2v25}) + r_7(N_{v25}^{c2} - e^{10/kT} N_0 N_{2v25}) + r_8(N_{v52}^2 - e^{10/kT} N_0 N_{2v25})$$

$$\frac{dN_{v25}^c}{dt} = r_7(e^{10/kT} N_0 N_{2v25} - N_{v25}^{c2}) + r_9(N_0 N_{v52} - N_0 N_{v25}^c) - r_{10} N_0 N_{v25} + r_{11} N_0 N_{v6} - TN_{v25}^c + rF Z_{23} \Psi (N_{2v3} - \frac{g_{2v3}}{g_{v25}} N_{v25}^L) - U(N_{v25}^c)$$

$$\frac{dN_{v25}^L}{dt} = Z_{23} \Psi (N_{2v3} - \frac{g_{2v3}}{g_{2v3}} N_{v25}^L) - TN_{v25}^L + rF[r_7(e^{10/kT} N_0 N_{2v25} - N_{v25}^{c2}) + r_9(N_0 N_{v52} - N_0 N_{v25}^c) - r_{10}(N_0 N_{v25}^c) + r_{11} N_0 N_{v6}] - U(N_{v25}^L)$$

$$\frac{dN_{v6}}{dt} = r_8(e^{10/kT} N_0 N_{2v25}^c - N_{v52}^2) + r_9(N_0 N_{v25}^c - N_0 N_{v52}) - r_{10} N_0 N_{v52} + r_{11} N_0 N_{v6} - YN_{v52}$$

$$\frac{dN_{v6}}{dt} = r_{12}(e^{113/kT} N_0 N_{v3} - N_0 N_{v6}) - 2r_{11} N_0 N_{v6} + r_{10} N_0 (N_{v25} + N_{v52}) - XN_{v6}$$

$$N_0 = K - [N_{v3} + N_{2v3} + N_{3v3} + N_{2v25} + N_{v25}^c + N_{v25}^L + N_{v52} + N_{v6}]$$

where

Ψ = 16 micron laser

Φ = input CO_2 laser

N_i = number density of particular energy level.

where

$$K = \sum_{i=0}^{9} N_i(t=0)$$

and we define the following constants

$$Q = \frac{h\nu_0 N^0 B_{23} W}{\bar{\nu}}$$

$$P = \frac{C \ln r_1 r_2}{2L\bar{\nu}}$$

$$Z_{11} = \Omega \frac{\nu_0^1}{\nu_0} \frac{B_{12} V}{c\bar{\nu}}$$

$$Z_{23} = \Omega \frac{\nu_0^1}{\nu_0} \frac{B_{23} W}{c\bar{\nu}}$$

$$r_i = k_i N^0/\bar{\nu}$$

(Collisional reaction rate k_i is defined by

$$\frac{dN_k}{dt} = k_{i1} N_i N_j - k_{i2} N_i N_k$$

for a process such as

$$CH_3F(N_i) + CH_3F(N_k) \rightleftarrows CH_3F(N_i) + CH_3F(N_j) + \hbar\nu$$

from the equilibrium condition

$$\frac{K_{i1}}{K_{i2}} = \frac{[CH_3F(N_i)CH_3F(N_j)]}{[CH_3F(N_i)CH_3F(N_k)]} = e^{\hbar\nu/kT})$$

T = $r/\bar{\nu}$ rotational relaxation

RF = % relaxation between two V_{25} rotational levels.

If levels are of different species RF = 0.

U,Y,X = collisional depopulation with diluent gas for that particular level.

Initial conditions on the vibrational level populations are given by Boltzmann statistics; while the initial condition on the 16 micron laser is given by the

spontaneous emission. The following parameters are used in the above definition:

h = Plancks constant = 6.626×10^{-27} erg sec

ν_0' = frequency of 16 micron Laser

ν_0 = frequency of CO_2 Laser

B_{12} = Einstein stimulated emission coefficient for ground to V_3 transition.

B_{23} = Einstein stimulated emission coefficient for $2V_3$ to V_{25} transition.

A_{23} = Einstein spontaneous emission coefficient for $2V_3$ to V_{25} transition.

N^0 = Population of the ground state rotational level which is optically pumped.

$\bar{\nu}$ = collisional frequency

W = methyl fluoride lineshape at 16 microns

V = overlap between pumping lineshape and absorbing lineshape.

Ω = Max power per unit area for CO_2 pumping laser

c = velocity of light in vacuum 3×10^{10} cm sec^{-1}

$r_1 r_2$ = mirror reflectivities

l = laser length (cm)

The effect of tuning the laser around the methyl fluoride line is contained within the constant V. From the quoted absorption coefficient the overlap intergal may be evaluated numerically.[30-32] Using equation A1, (Appendix A) we see this gives a distance between the CO_2 and absorbing methyl fluoride line of approximately

1.61×10^{-2} cm^{-1}. This agrees favorably with the predicted distance from the theoretical spectrum of figure 17. The laser used in this experiment was a Q-switched, mode-stablized laser. By changing the frequency difference between CO_2 and methyl fluoride lines, the effect of tuning the transition to exact resonance may be simulated. Figure 21 shows the predicted position for a common Q-switched laser relative to methyl fluoride (Appendix A). This situation may be changed however by changing $(\nu-\nu_c)$. An experimental condition such as figure 22 may be simulated by bringing the CO_2 laser line very close to the methyl fluoride transition, or moving it across the methyl fluoride transition in time.

The Einstein coefficients for the $V_3 = 2$ to $V_{25} = 1$ transition may be varied to see how sensitive laser operation is to them. As a first guess (see Appendix B) we choose $B_{23} = 4.58 \times 10^{19}$ $cm^3 J^{-1} sec^{-2}$. The collisional rates are given in figure 19 and diluent collision rates will either be taken from experiment or assumed.[45,49]

The rotational relaxation rate of methyl fluoride, as previously stated, has been measured to be on the order of 10^3 collisions. We will use 1000 collisions. All calculations are carried out at 300 degrees Kelvin. Only these parameters which may be easily met in the laboratory will be considered thus eliminating exotic experimental set-ups to check the computer predictions.

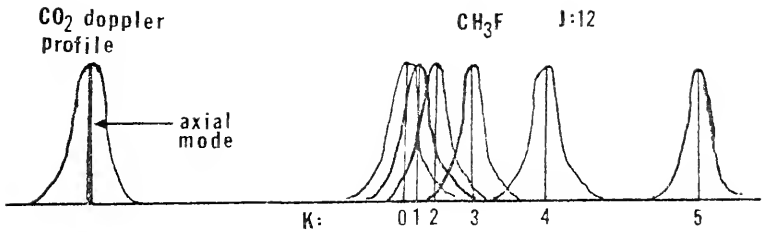

Figure 21. CO_2 and methyl fluoride lineshapes.

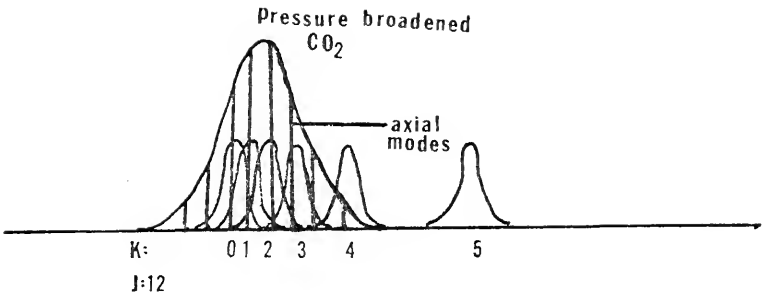

Figure 22. Broadened CO_2 in resonance with methyl fluoride.

CHAPTER V RESULTS

Numerical solutions of the equations described in the last chapter were carried out at the University of Florida on an I.B.M. 360-75 computer. The numerical technique employed was Hamming's modification of the Milne predictor -corrector method. A fourth order Runge-Kutta method is used to generate the first time-increment solution since the predictor - corrector method is not self-starting. Hamming's method is a stable fourth order integration procedure which has the advantage of a variable step size. This saves computing time without sacrificing accuracy.

The accuracy for all the results was kept between one part in 10^3 to one part in 10^4. This is better than actually required; however it facilitates faster overall integration since solutions were not allowed to start diverging at any point. The time step was between .5 and .01 measured in units of time where one unit was the time for one collision. The predictor - corrector method was able to bisect the time step up to 10 times if required to obtain the specified accuracy.

The first question which needed to be answered was what parameters to start the model with since there are

a large number for which threshold and subsequent lasing would not occur. This depends on the Einstein coefficient as was discussed in Chapter IV. Figures 23 and 24 show the reflectivity needed at a particular pressure to satisfy the Schawlow-Townes condition. The population inversion may be estimated from the thermal population of the lower laser level since little additional population is expected during the first several collisions. The three curves are drawn for the Einstein coefficients: (L = 100cm)

A; $B_{12} = 4.58 \times 10^{19}\ cm^3 J^{-1}\ sec^{-2}$

B; $B_{12} = 4.58 \times 10^{20}\ cm^3 J^{-1}\ sec^{-2}$

C; $B_{12} = 4.58 \times 10^{18}\ cm^3 J^{-1}\ sec^{-2}$.

All numerical work was performed for case A although if the actual B_{12} is anywhere in the above range, the equations will take the same form by picking a point on the appropriate curve. The laser output however will decrease as the reflectivity increases so that for reflectivity above .99 little output will be expected. It can be seen that case C is more or less a limiting case for practical application.

Unless otherwise stated the conditions and parameters were as follows:

Pressure = 10 torr

Pump power = 10 watts/cm^2

Pump duration = CW

Reflectivities = 100%, 98%

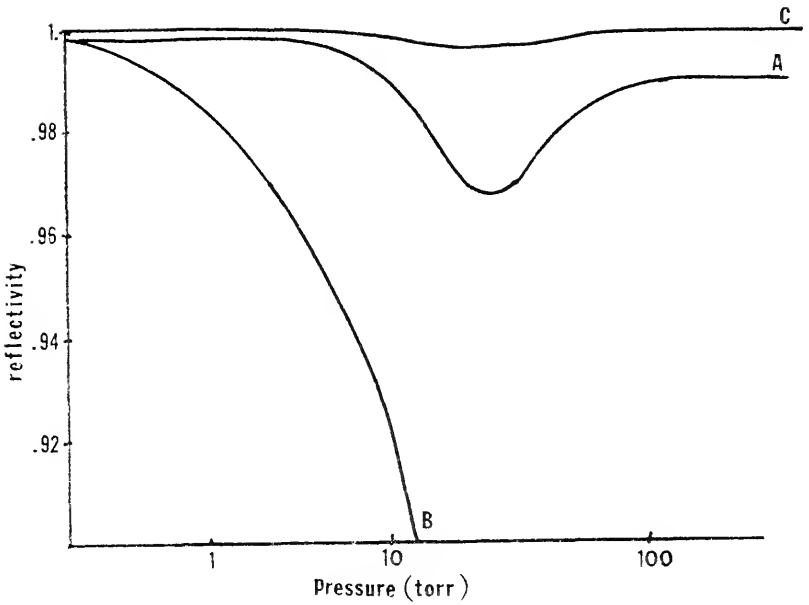

Figure 23. Schalow-Townes condition for inversion of 5×10^{-3} (L= 100cm).

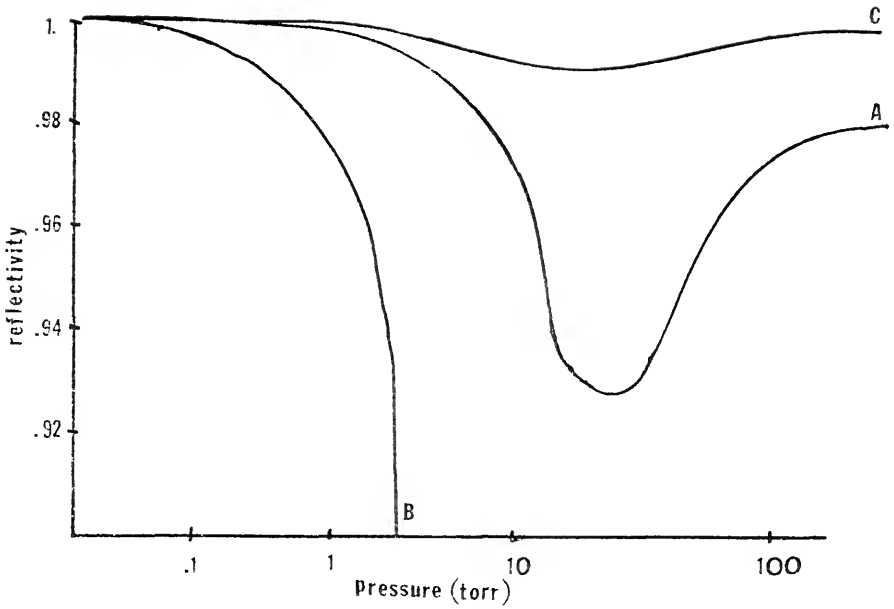

Figure 24. Schalow-Townes condition for inversion of 1×10^{-2}, (L= 100 cm).

Laser length = 200 cm

Pump J,K; $J^1 = 12$ $K^1 = 2$

Laser transitions (lower) J,K; $J^{11} = 12$, $K^{11} = 2$

Distance between CO_2 and CH_3F linecenters

$= 1.62 \times 10^{-2}$ cm^{-1}

Rotational relaxation = 10^3 collisions

Diluent relaxation = none.

Cases of departure from these conditions will be dealt with as necessary. Figure 25 shows the laser pulse as it first starts to develop for 250 nsec after being pumped by a kilowatt CO_2 laser pulse for 50 nsec. Notice that the laser does not immediately start to amplify after threshold is reached, but waits several hundred nanoseconds before the pulse starts to curve upwards again. This is due to the relatively small Einstein coefficient ($\sim 10^{19}$ J^{-1} cm^3 sec^{-2}) for the $2V_3$ to V_{25} transition. In studying the populations of each level in the model during the first few collisions several things were apparent. The relatively strong absorption coefficient ($.018 cm^{-1} torr^{-1}$ for P(20)) caused the ground to V_3 transition to saturate within a few collisions. This strongly limited the amount of energy in the CO_2 pulse which was utilized, since after saturation nearly all the laser pulse propagates through the laser medium as a bleaching wave. Increasing the power of the pump CO_2 laser for this type of situation was found to have little effect on output or populations as might be expected.

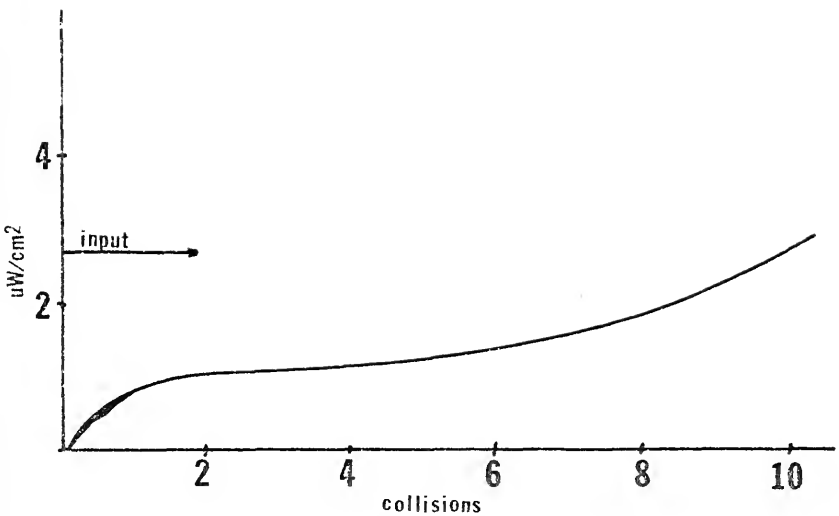

Figure 25. CH_3F pulse following threshold.

In the figures presented for energy level populations, the following symbols are used.

SYMBOL	ENERGY LEVEL
2	V_3
3	$2V_3$
4	$3V_3$
5	V_{41}
6	$2V_{25}$
7	V_{25}^{c} collisionally filled level
8	V_{25}^{L} laser level
9	V_{52}
0	V_6

Figures 26a through 261 show the results of pumping methyl fluoride with a megawatt 100nsec CO_2 laser. The resulting 16 micron laser output has a peak intensity of approximately 5 watts/cm^2 in 10^{-6} sec. Notice that only 3.4 microseconds elapse between pump and laser output. The maximum population inversion occurs in only 20 collisions and decays nearly linearly for the next 150 collisions. The population of V_3=1 level saturates immediately and decays via V-V collisions. The populations of the V_3= 1,2,3 levels all peak with a phase delay corresponding to the V-V equilibrium rate. Notice that the maximum population of each level is less than the level previous thus indicating the collisional equilibrium described earlier. This is not true for the V_{25} level which is also populated by radiative transitions. It is

interesting to note that although the V_{52} level is not populated by radiative transitions, it is always in equlibrium with the V_{25} level. This is due to the fact that both levels form a hybrid pair and are different linear combinations of the same two levels. These levels are degenerate and the resulting pair are in Fermi resonance and are thus split by only $2cm^{-1}$. In contrast to these figures consider figures 27a through 27l. This set show response to a 5 watt CW CO_2 laser. Notice that the 16 micron laser takes nearly 2.5 times longer to form its pulse, and the pulse is nearly 7 watts. The long phase delay is understood if it is recalled that lasing occurs from the V_3= 2 level. By pumping with only 5 watts it takes nearly 100 collisions to saturate the ground to V_3 transition and thus population in V_3= 2 does not peak until 180 collisions after CO_2 pumping is initiated. The V_{25} level is being collisionally populated during this time; however the figure clearly shows that the rate for collisional population is much smaller than that for radiative.

This explains why the population inversion has such a slow rise time and rapid decline, as compared with the previous figure. An important difference to note between CW and short pulsed pumping is that in the CW case the upper vibrational levels are collisionally populated much more than the pulsed case. This is because of the long phase delay of the output laser thus requiring levels

```
PRESSURE TORR
10.000

PUMP J,K  LOWER LASER LEVEL J,K  G0/GV3, G2V3/GV25
    12     2      12     2       1.0000     1.0000

NUMBER DENSITY NO-CM-3
          0.9558E 16


EINSTIEN COEFS CM3 J-1 SEC-2 B25,A25,B12
     0.4580E 20      0.9281E 03      0.6800E 24

COLLISION FREQUENCY SEC-1
     0.4390E 08

OVERLAP INTEGRAL FOR TWO LORENTZEN BROADNED LINES
LINE CENTER DISTANCE-HALF WIDTHS METHYL FLUORIDE AND CO2SEC-1
        0.4850E 09      0.6000E 08      0.3000E 06

OVERLAP INTEGRAL L-L SEC
          0.4064E-10

CO2 LASER IMPUT WATTS/CM2  DURATION IN          COLLISIONS
     0.1000E 07      4.000

Z11...Z23...G23...S
     0.2099E 04      0.5796E 02      0.2065E 01      0.1846E-06

DILUENT COLLISIONAL DEPOPULATION     ROTATIONAL RELAXATION
NL25-N52-N6-ROT, RELAX,#COLLISIONS-1
          0.0            0.0            0.0            0.001

%RELAXATION BETWEEN NL25-N25,A FN OF J,K.
          1.0000

MIRRIOR REFLECTIVITIES, LASER CAVITY LENGTH CM
    1.000  0.980       200.000

P=     -0.0345
```

Figure 26a. Parameters.

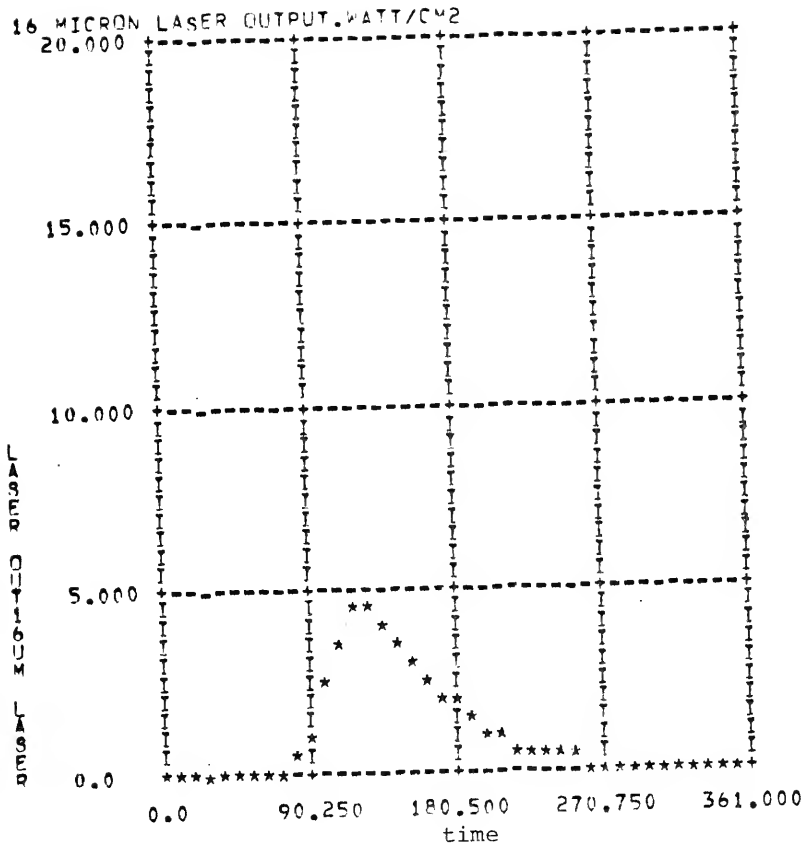

Figure 26b. Methyl fluoride laser.

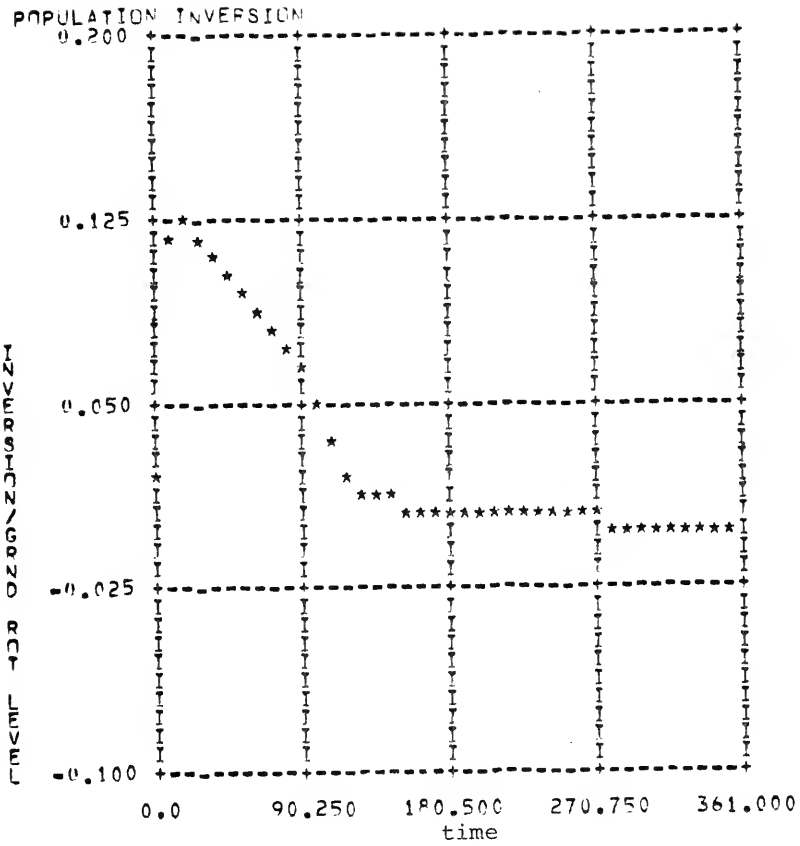

Figure 26c. Population inversion.

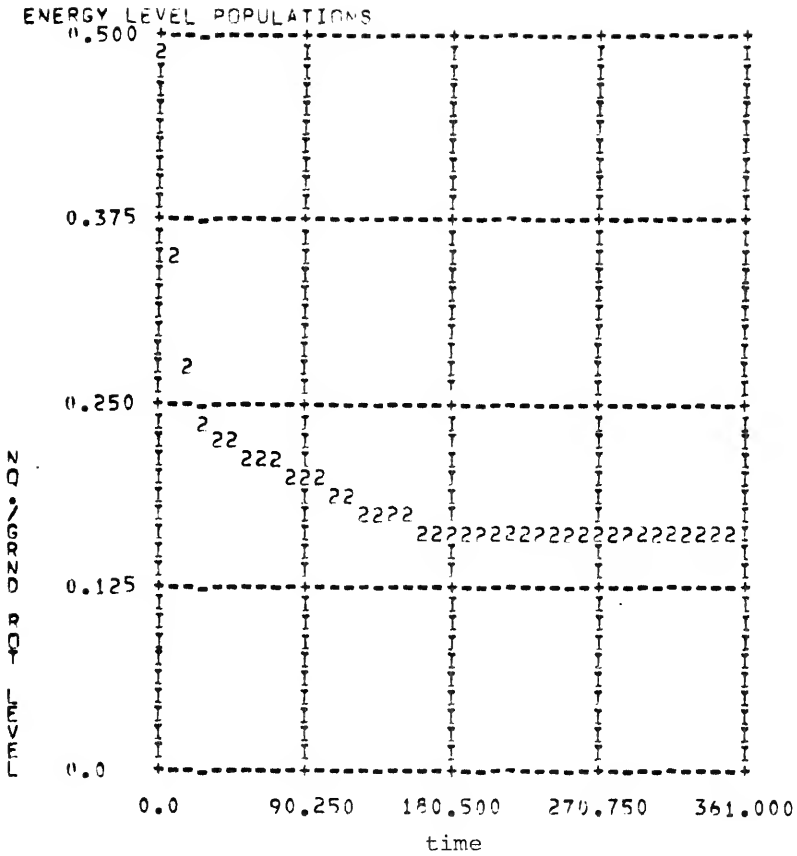

Figure 26d. Population of V_3.

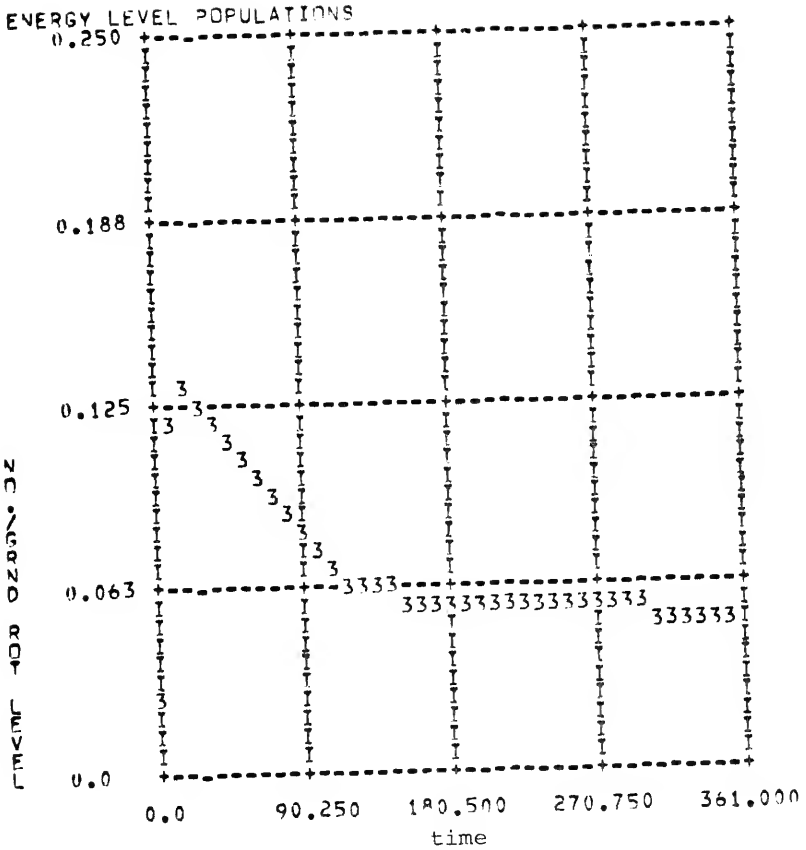

Figure 26e. Population of $2V_3$.

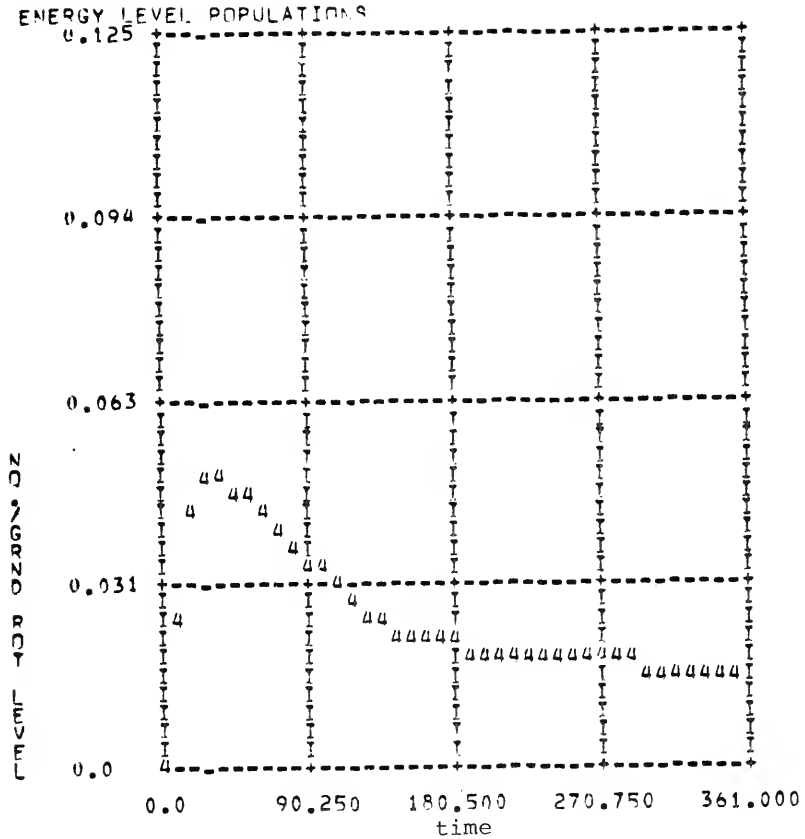

Figure 26f. Population of $3V_3$.

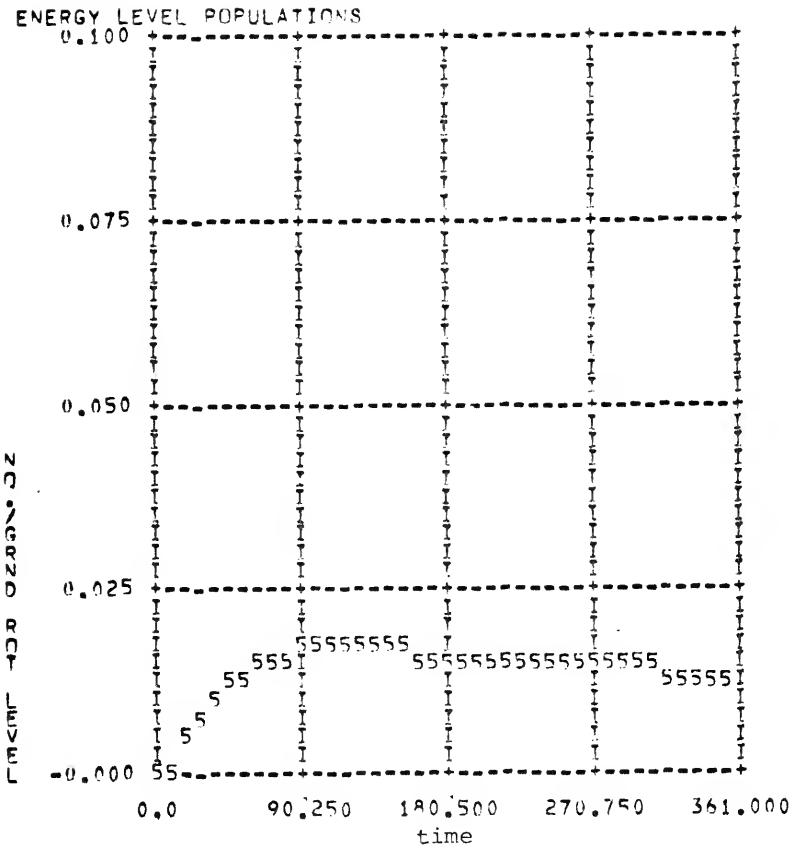

Figure 26g. Population of V_{41}.

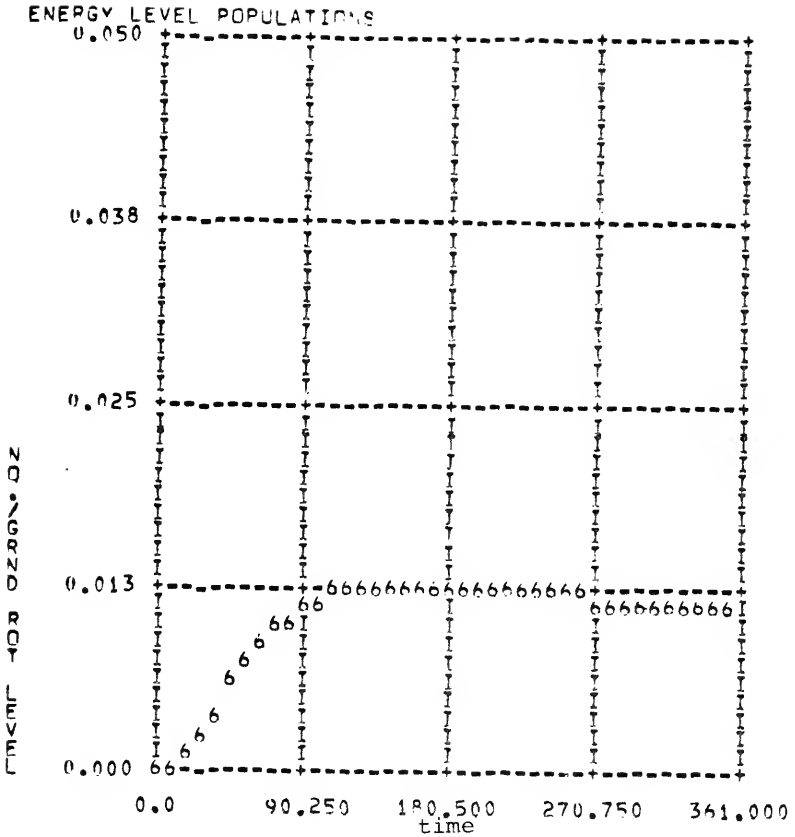

Figure 26h. Population of $^2V_{25}$.

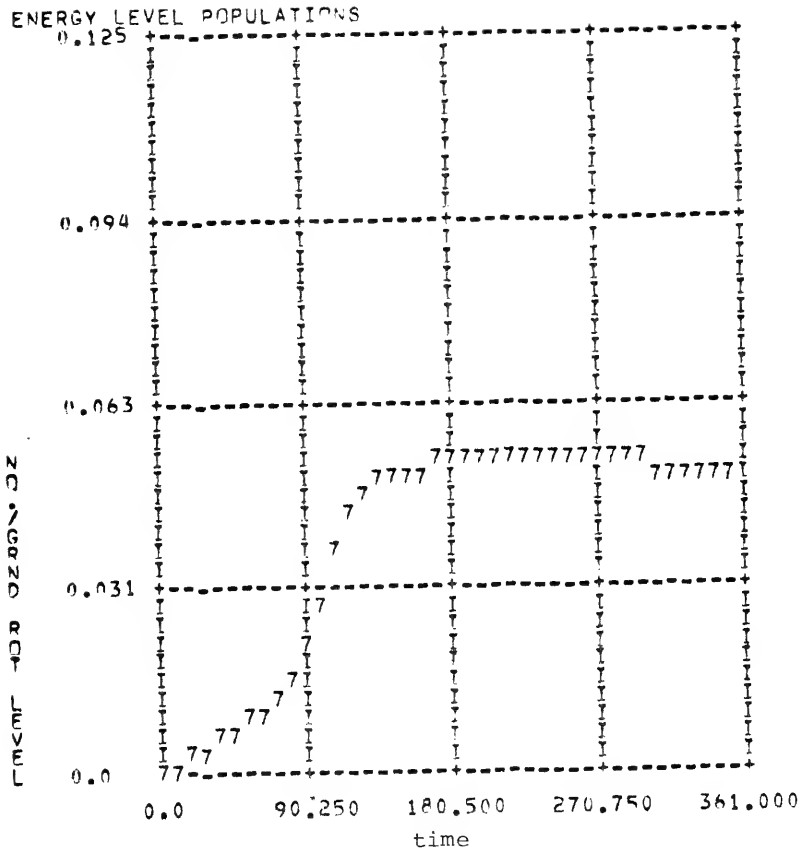

Figure 26i. Population of V_{25}^{C}.

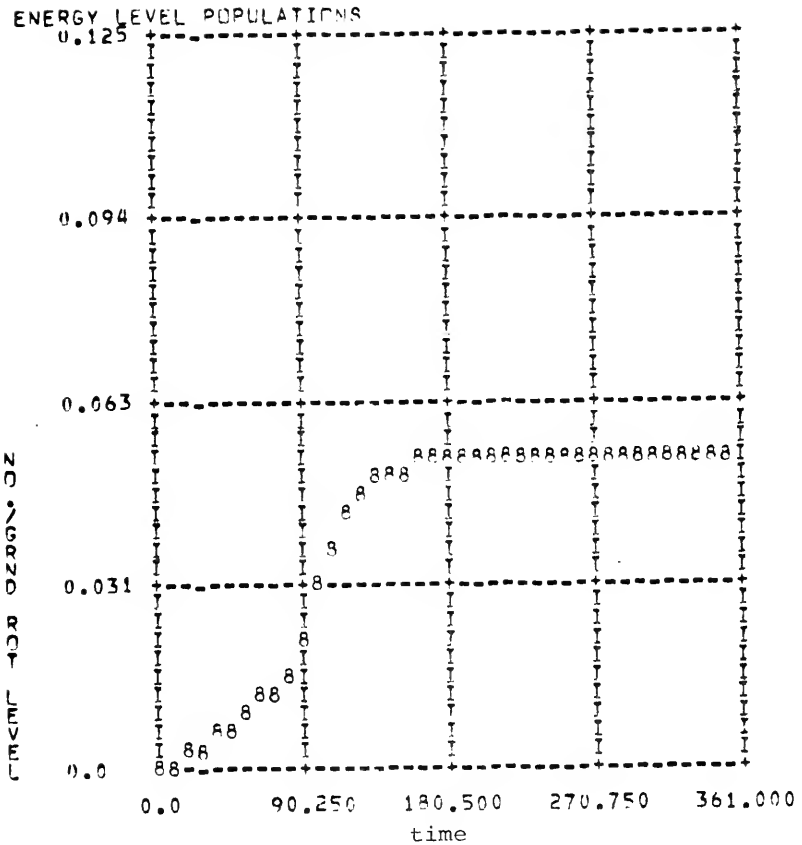

Figure 26j. Population of V_{25}^{1}.

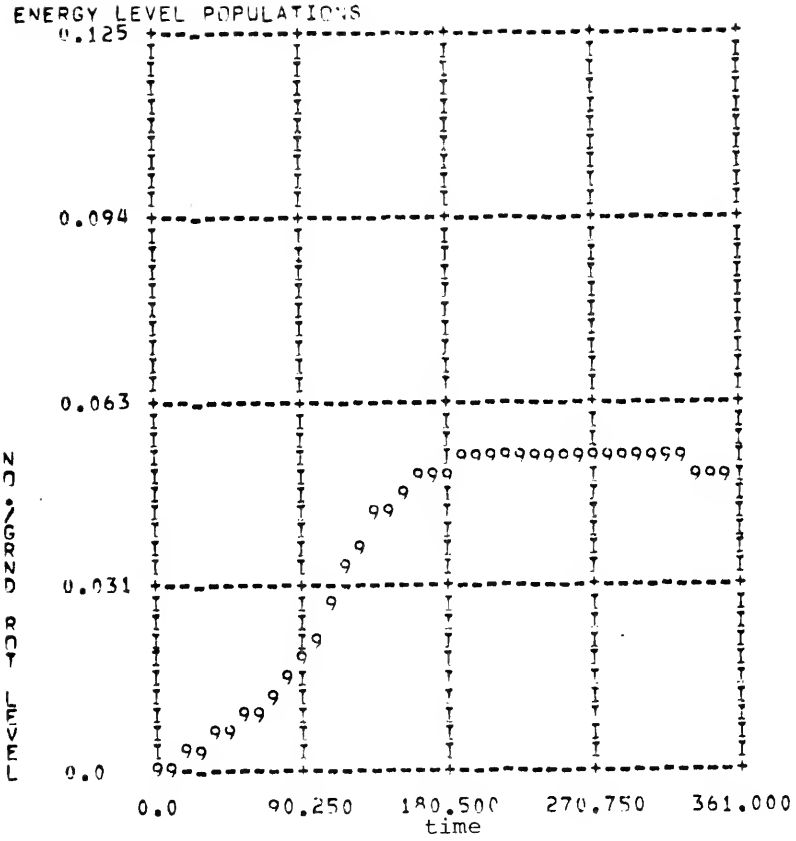

Figure 26k. Population of V_{52}.

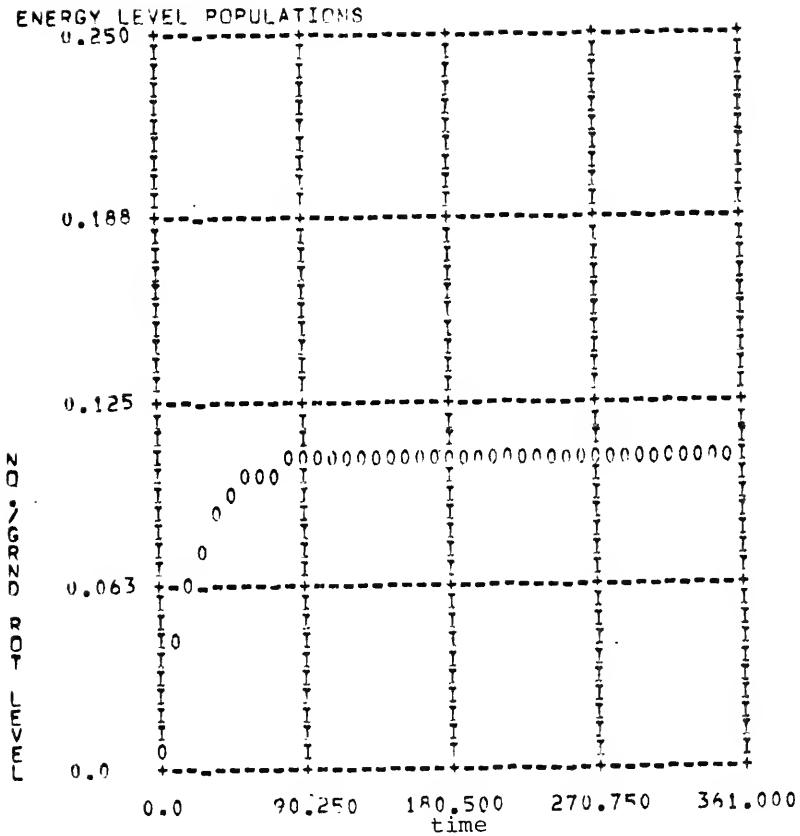

Figure 261. Population of V_6.

```
PRESSURE TORR
10.000
PUMP J,K  LOWER LASER LEVEL J,K  G0/GV3, G2V3/GV25
   12  2      12  2       1.0000     1.0000

NUMBER DENSITY NO-CM-3
          0.9558E 16

EINSTIEN COEFS CM3 J-1 SEC-2 B25,A25,B12
     0.4580E 20      0.9281E 03      0.6800E 24

COLLISION FREQUENCY SEC-1
     0.4390E 08

OVERLAP INTEGRAL FOR TWO LORENTZEN BROADNED LINES
LINE CENTER DISTANCE-HALF WIDTHS METHYL FLUORIDE AND CO2SEC-1
          0.4850E 09          0.6000E 08          0.3000E 06

OVERLAP INTEGRAL L-L SEC
          0.4064E-10

CO2 LASER IMPUT WATTS/CM2  DURATION IN          COLLISIONS
     0.5000E 01      361.000

Z11...Z23...Q23...S
     0.1049E-01      0.2809E-03      0.2045E 01      0.3692E-01

DILUENT COLLISIONAL DEPOPULATION    ROTATIONAL RELAXATION
NL25-N52-N6-ROT. RELAX:#COLLISIONS-1
          0.0          0.0          0.0          0.001

%RELAXATION BETWEEN NL25-NG25.A FN OF J,K.
          1.0000

MIRRIOR REFLECTIVITIES, LASER CAVITY LENGTH CM
     1.000   0.930        200.000

P=     -0.0345
```

Figure 27a. Parameters.

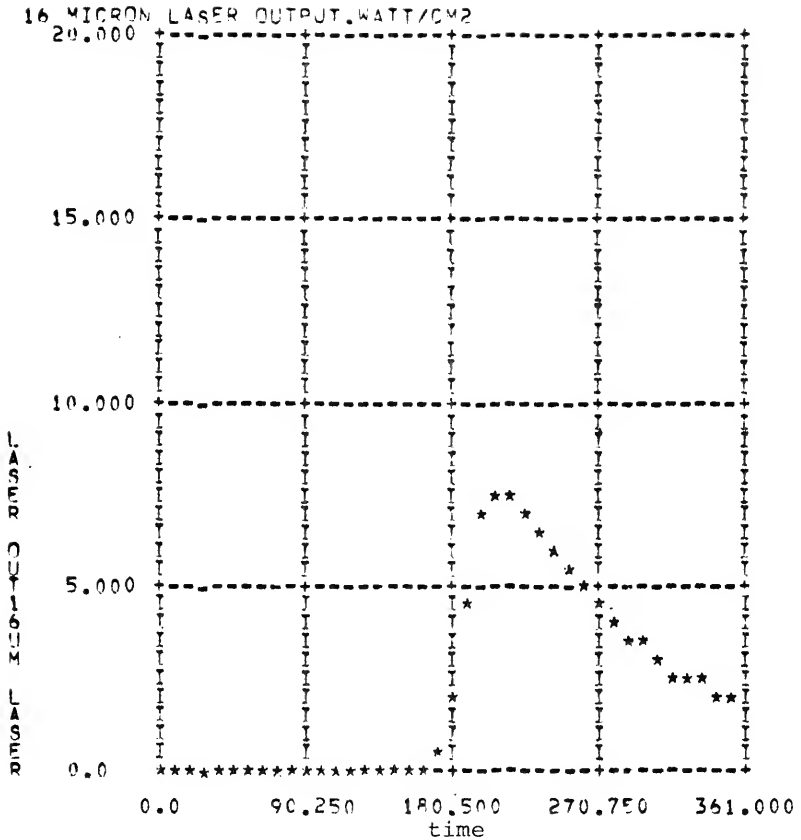

Figure 27b. Methyl fluoride laser.

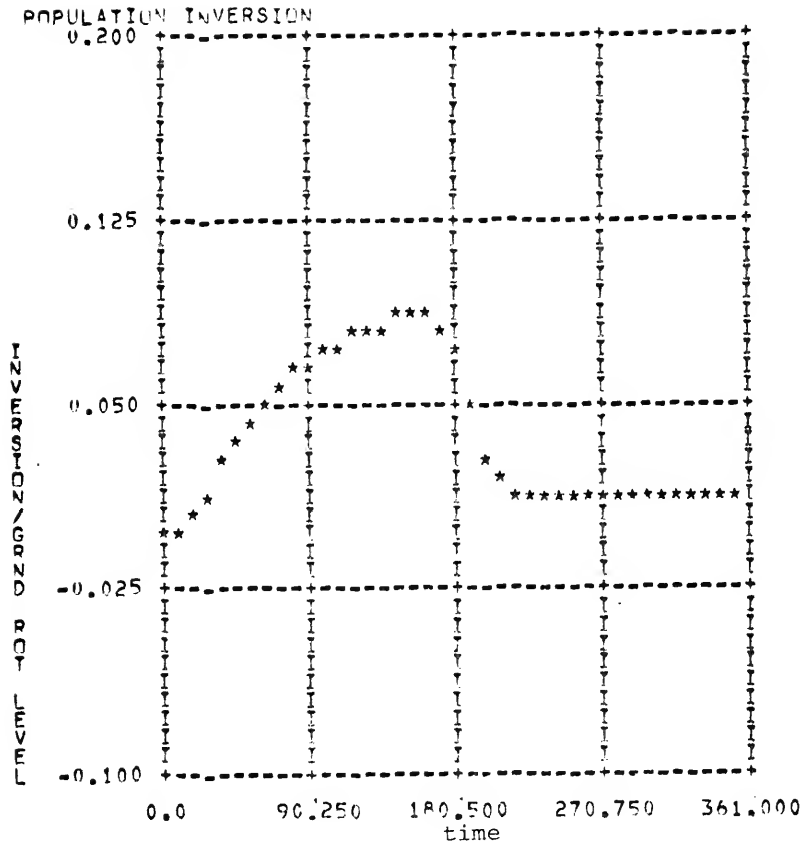

Figure 27c. Population inversion.

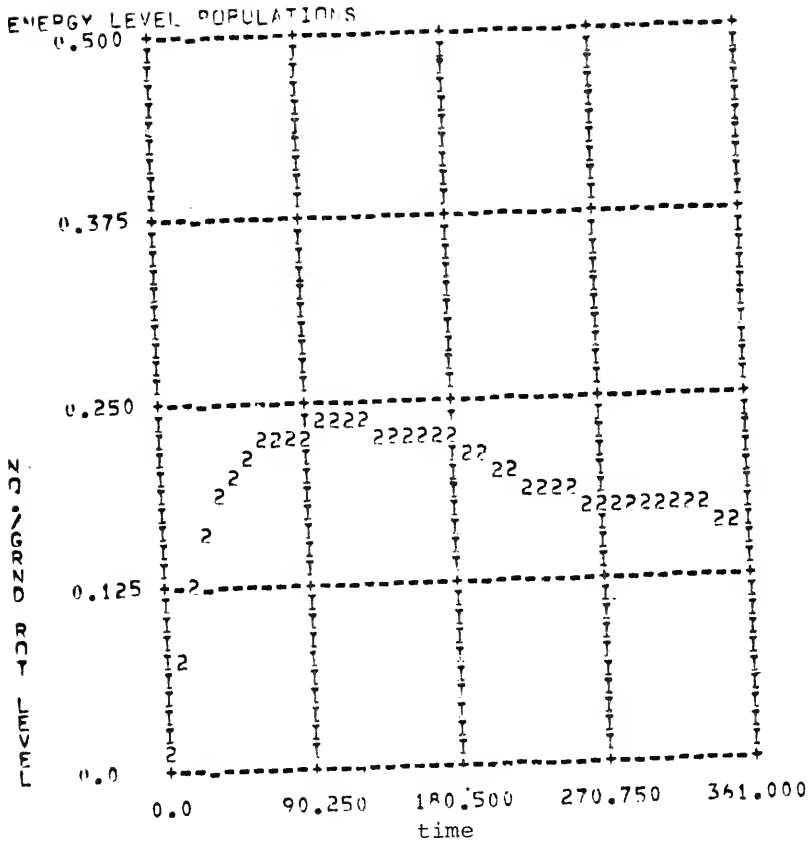

Figure 27d. Population of V_3.

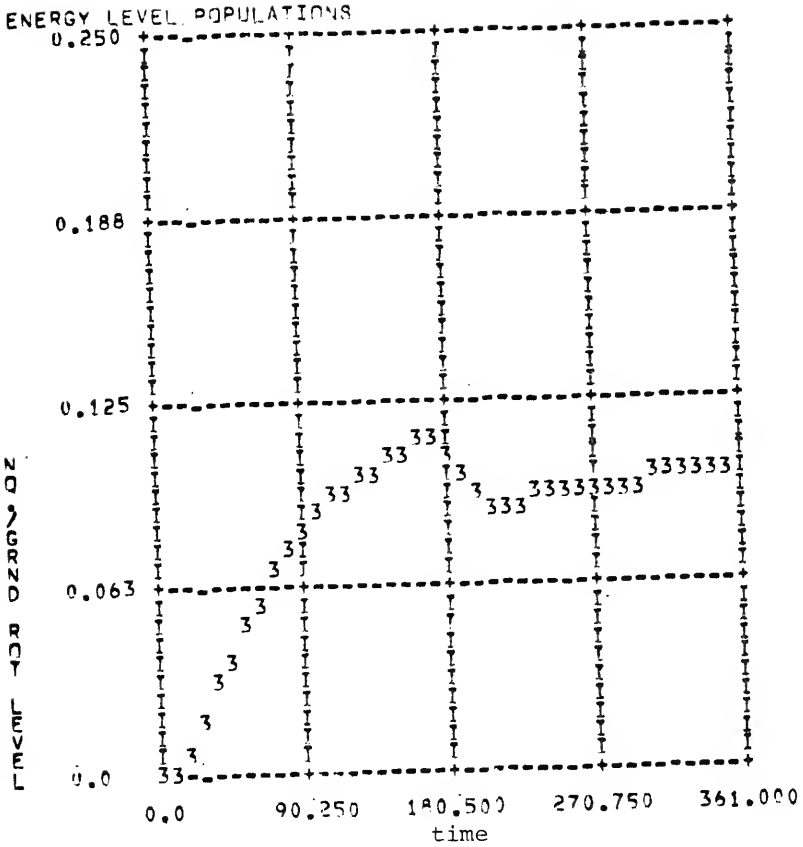

Figure 27e. Population of $2V_3$.

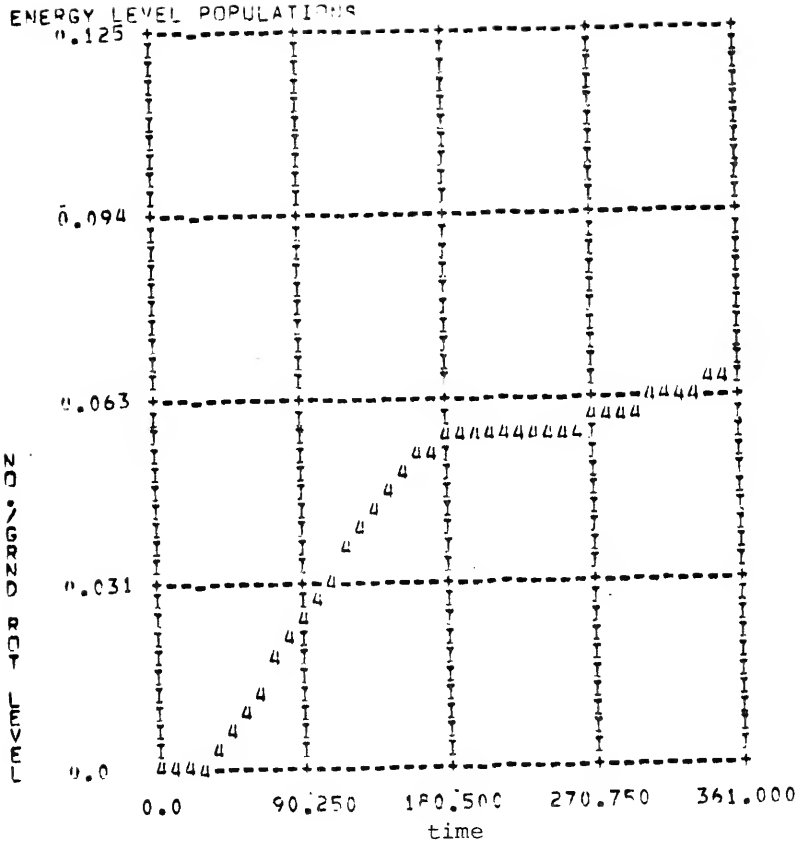

Figure 27f. Population of $3V_3$.

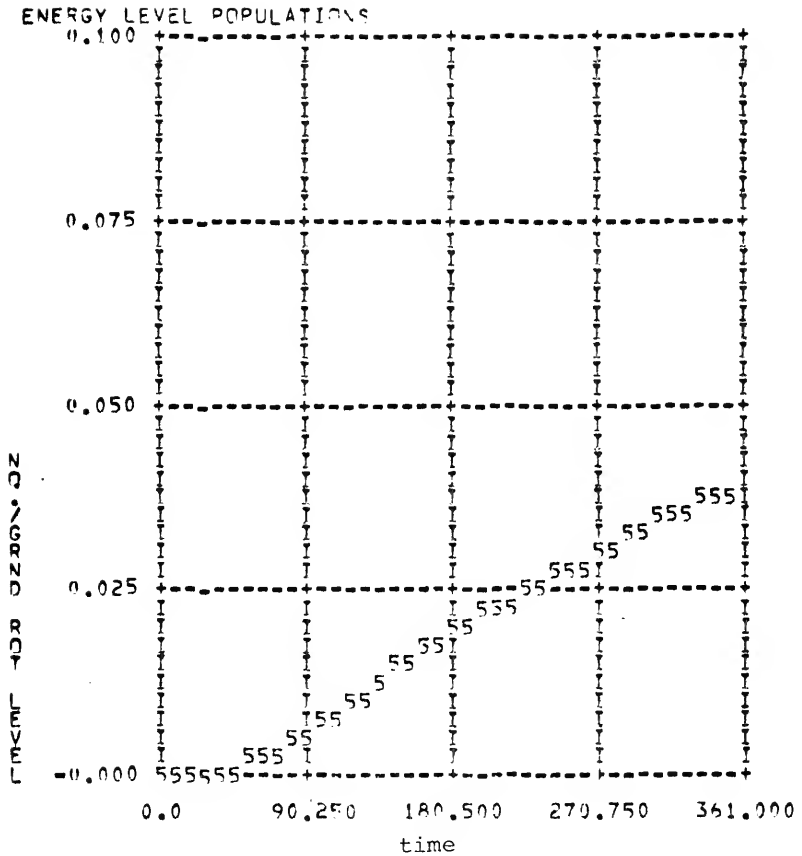

Figure 27g. Ppoulation of V_{41}.

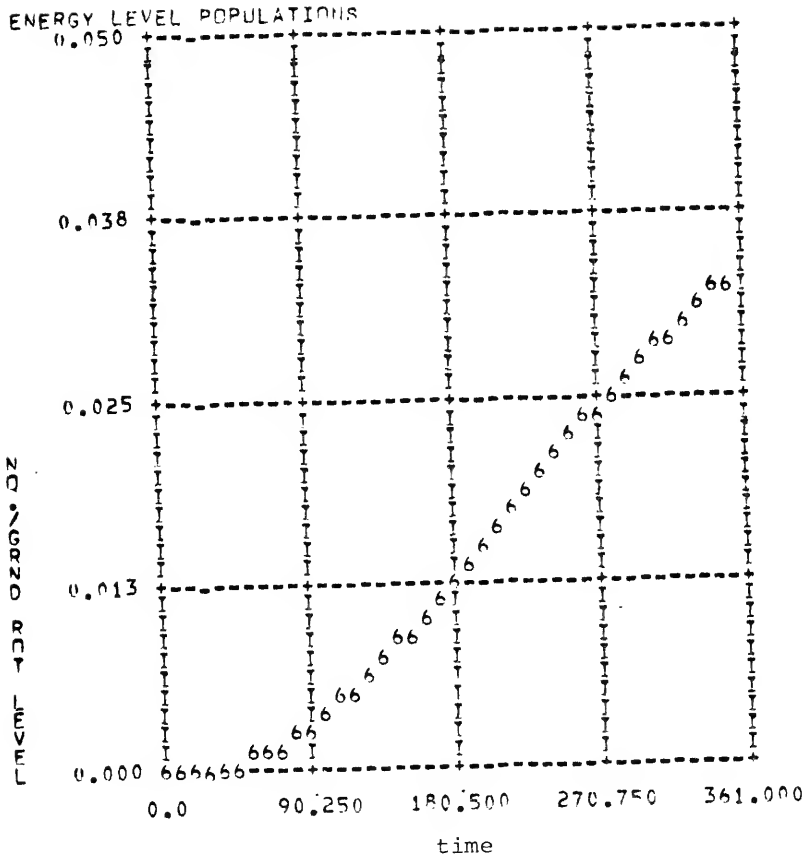

Figure 27h. Population of $^2V_{25}$.

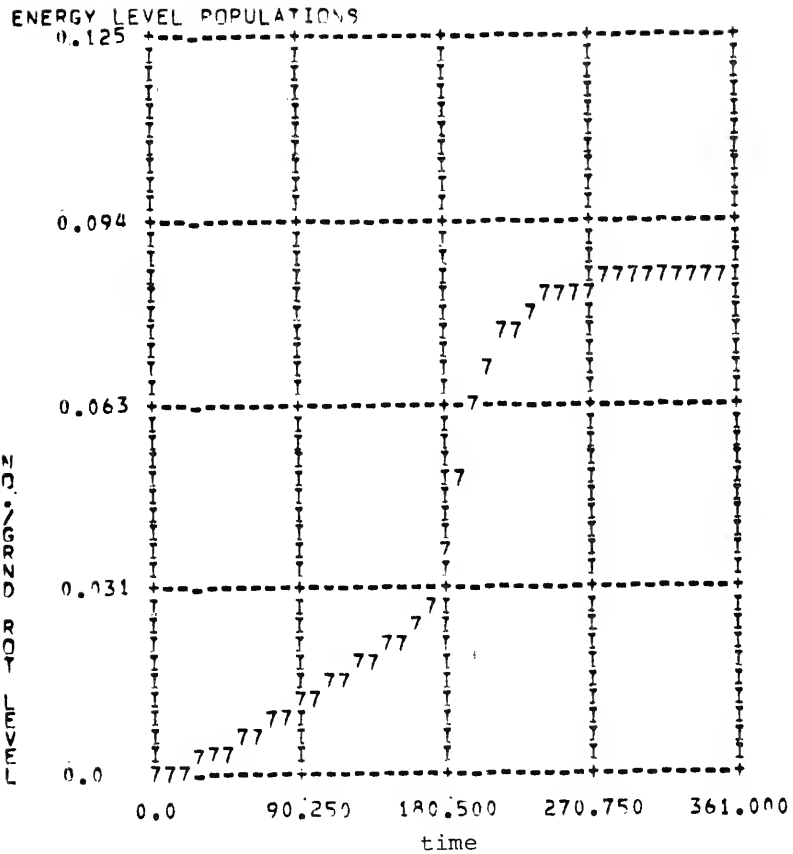

Figure 27i. Population of V_{25}^{C}.

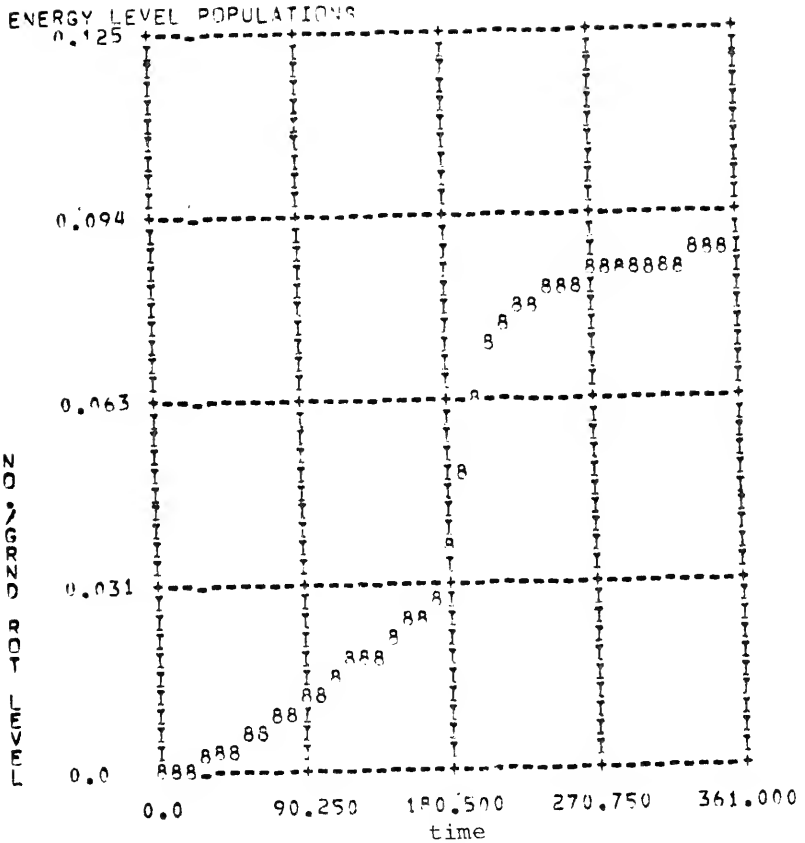

Figure 27j. Population of V_{25}^{1}.

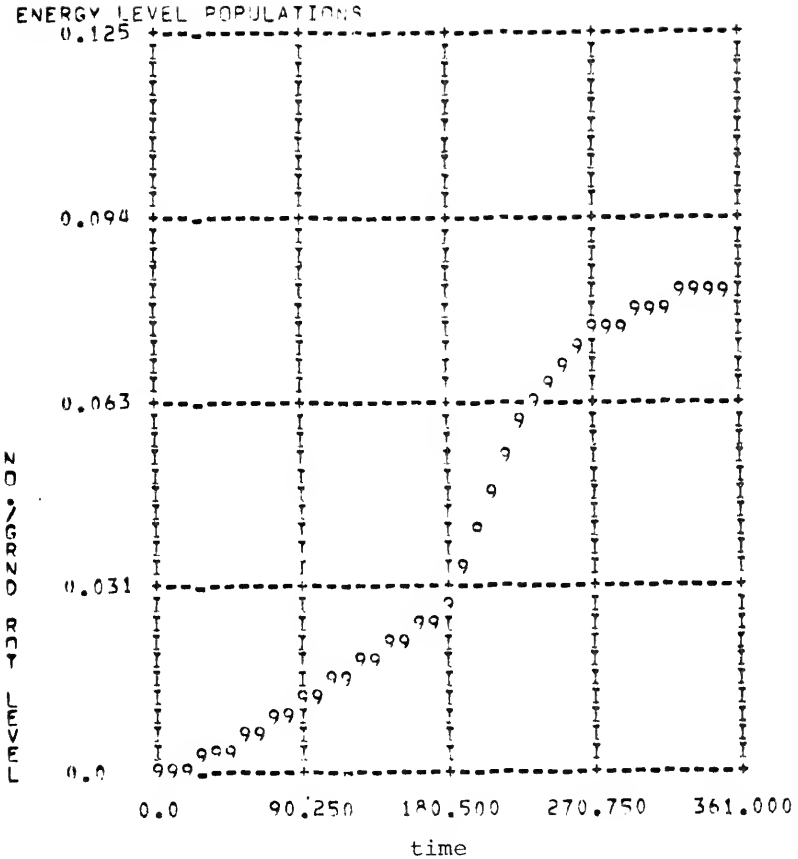

Figure 27k. Population of V_{52}.

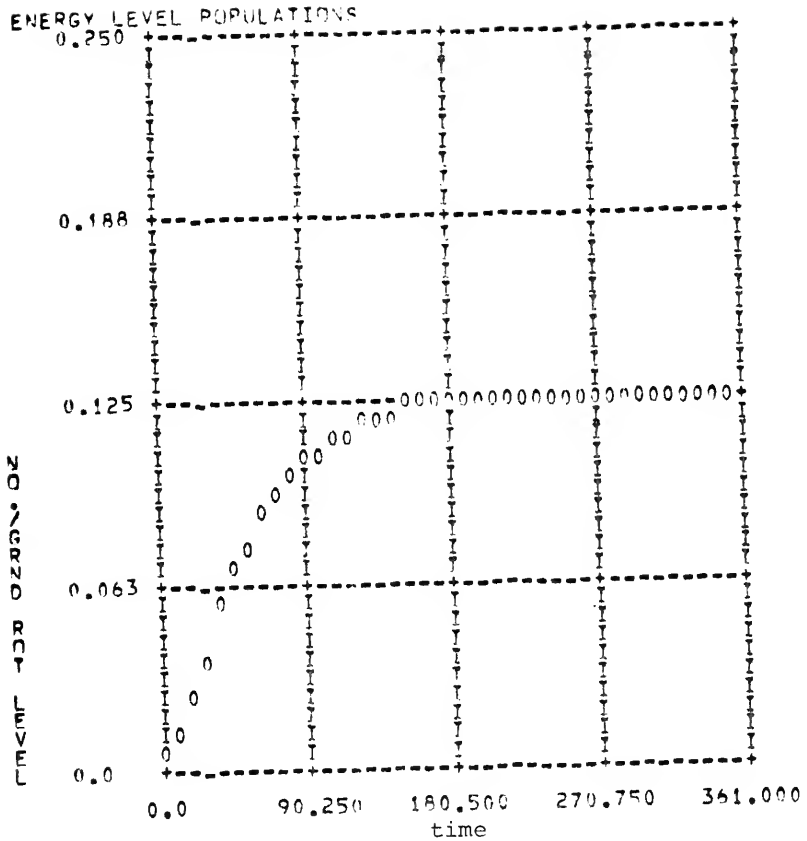

Figure 271. Population of V_6.

to remain in equilibrium. Thus during CW operation the lower laser level (V_{25}) is populated much higher before lasing thus reducing the population inversion. The explanation of why the CW case has higher output and lower population inversion is revealed by comparing the two figures for each case (figures 26c, 27c). Although the inversion for the pulsed input reaches a higher value, it also takes nearly three times as long to release its energy. The power output of the CW pump is then understandably higher since the time rate of change of energy released is higher.

Of the 22 different parameters sets run numerically, figures 26 and 27 are representative for all. As might be expected there was no magic combination of parameters which greatly increased laser output, although all 22 combinations yielded a 16 micron laser of at least several watts/cm^2. The figures for all 20 other combinations will not be shown since they resemble so strongly those of 26 and 27 that little additional information would be gained. (See Appendix C).

Figure 28 indicates the efficiency for different types of carbon-dioxide lasers. The parameter I is a measure of energy (I = .023mJ). The first thing one notices about this figure is that all points fall more or less along a straight line which peaks around log(I)=3 and sharply drops off below that. This represents the

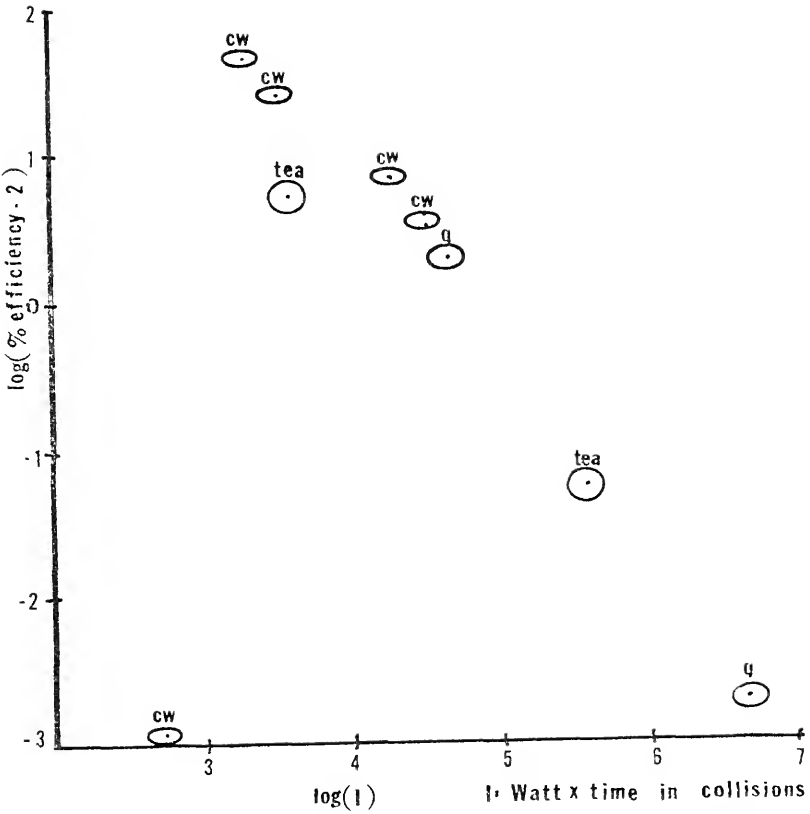

Figure 28. Effect of CO_2 pumping on 16 micron laser efficiency.

amount of energy to keep the ground to V_3 transition saturated while the other vibrational levels are becoming populated, without creating a bleaching wave. Notice that in all cases, where pulse time lengthens, efficiency increases. As you demand less power from the system, efficiency is able to get quite high. The points to the right to the peak have much higher output power than those to the left; however they also have much lower efficiency. Pulse times for all points are as follows:

tea; 100 nsec.

q-switch; 1 microsec.

CW; CW.

Quantum efficiency would be at 1.8 on the ordinate. Thus it is seen that a 16 micron laser with very high efficiency could be produced if one were content to use very low power pump CO_2 laser and get low power (several watts in several microseconds) output. This does not mean however that high radiation density cannot be achieved at 16 microns. One may still operate a large volume methyl fluoride cavity and focus the beam to increase the power per unit area at the focal point.

CHAPTER VI CONCLUSION

The feasibility of producing a 16 micron laser from methyl fluoride has been demonstrated in this paper. The mechanism for energizing the methyl fluoride molecule is through optical pumping by the P(20), 9.6 band carbon-dioxide laser which is known to absorb strongly into methyl fluoride.[25, 31, 32] Numerical work was done on a semi-classical model which showed this technique was indeed possible. The success of this type of approach is due to the large amount of experimental work carried out on methyl fluoride previously, thus documenting absorption coefficient, absorbing line, and collisional rates.[25, 30, 31, 35, 41, 42, 44, 45-54]

The methyl fluoride laser described herein is characterized by high reflectivity and pressure, and long gain length. This is expected, since the amplification is less than .51%/cm. This does not however preclude the methyl fluoride laser from having substantial output or high efficiency. Output of from 5 to 20 watts/cm^2 in several microseconds was shown to be obtainable under several conditions and configurations.

Energy storage in methyl fluoride is small, (approximately 31.45 $mJL^{-1}torr^{-1}$) so that methyl fluoride

may be used more effectively as an amplifier of 16 micron radiation than an oscillator. This would be possible since small amounts of 16 micron radiation may be generated in crystals. The system envisioned might be similar to those used in fusion research. A small oscillator would feed radiation to a series of amplifiers which would provide a high intensity radiation field.

APPENDIX A

The overlap integral between the CO_2 lineshape and the methyl fluoride lineshape is shown below.

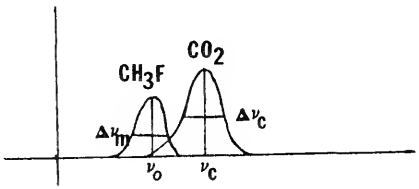

Assuming both lines are homogeneously broadened the overlap integral takes the form

$$V = \int_{-\infty}^{\infty} \frac{\Delta\nu_c \Delta\nu_m}{(2\pi)^2} \left[(\nu-\nu_0)^2 + \left(\frac{\Delta\nu_m}{2}\right)^2\right]^{-1} \left[(\nu-\nu_c)^2 + \left(\frac{\Delta\nu_c}{2}\right)^2\right]^{-1} d\nu$$

let $\omega = \nu-\nu_0 \quad \omega^1=\nu_c-\nu_0$

then the integral becomes $V = \frac{\Delta\nu_c \Delta\nu_m}{(2\pi)^2} I$

where

$$I = \oint \frac{d\omega}{(\omega^2 + A^2)((\omega-\omega^1)^2 + B^2)}$$

and

$$A = \frac{\Delta\nu_m}{2}, \quad B = \frac{\Delta\nu_c}{2}$$

This may be written as a contour integral and complete as shown. The integral has two simple poles at iA and $iB + \omega^1$.

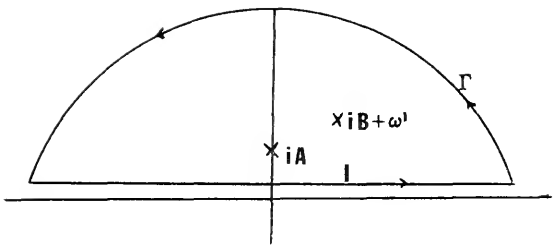

From the figure

$$\oint \frac{d\omega}{(\omega^2 + A^2)((\omega-\omega')^2 + B^2)} = I + \Gamma = 2\pi i \Sigma \text{residues}$$

however on Γ one may write

$$\omega = re^{i\theta}$$

and the integral vanishes as r^{-3} as $r \to \infty$. Thus the contribution along $\Gamma = 0$. We then evaluate the residue at each pole to yield the result

A1. $$V = \frac{1}{2\pi}\left[\left(\frac{\Delta\nu_c}{2}\right)^2 + \left(\frac{\Delta\nu_m}{2}\right)^2 + (\nu_c - \nu_m)^2\right]^{-1}(\Delta\nu_c + \Delta\nu_m)$$

where we assume that the frequency distribution is symmetric with respect to reflection in the origin. This is assumed because photons traveling to the right through the cavity see the frequency shifted up, while those traveling to the left see it shifted down. This is only strictly true for inhomogenously broadened lines. However the lineshape between the two is similar enough that little inaccuracy is introduced by assuming a Lorentzian lineshape.

APPENDIX B

The Einstein coefficients for stiumlated and spontaneous emission from the $V_3 = 2$ to V_2 or $V_5 = 1$ levels of CH_3F could be obtained from the measured integrated molar absorption coefficients from infrared intensity studies of the "hot-band" transition (V_2 or $V_5 = 1$ to $V_3 = 2$). Unfortunately, there have not been any such studies of the intensity of this transition. Hence, we are forced to estimate the intensity of this transition from some theoretical treatment of "hot-band" intensities. The most understandable treatment of this problem is in an unpublished preprint by Yao and Overend. They find that the matrix element for the transition dipole for a difference band is

$$\langle v_s, v_{s'}, v_{s''} \,|P'|\, v_s+1, v_{s'}-1, v_{s''}\rangle$$

$$= P_{ss'} \left(\frac{v_s+1}{2}\right)^{1/2} \left(\frac{v_{s'}}{2}\right)^{1/2} 1 + \frac{2P_s}{P_{ss'}} \{g_3(sss' + g_4(sss')\}$$

$$+ \frac{2P_{s'}}{P_{ss'}} \times \{g_3(s's's) + g_4(s's's)\}$$

and the intensity or Einstein coefficient is thus proportional to the square of this value. Here $P_{ss'} = \partial^2 P/\partial Q_s \partial Q_{s'}$, is the mixed second derivative of the dipole

moment P and is part of the "electrical anharmonicity" of the molecule, s and s' refer to the vibrational modes that are involved, $P_s = \partial P/\partial Q_s$ and $P_{s'} = \partial P/\partial Q_{s'}$, and the g_3 and g_4 functions are related to the mechanical anharmonicities

$$g_3\ (sss') = \omega_s \omega_{s'} g_1$$
$$g_4\ (sss') = 2\omega_s^2 g_1$$
$$g_1\ (sss') = -(k_{sss'}/\omega_s)\ (4\omega_s^2 - \omega_{s'}^2)^{-1}.$$

Here ω_s and $\omega_{s'}$ are the harmonic frequencies involved, and $k_{sss'}$ is the mechanical anharmonicity potential constant.

Since we do not know enough about the CH_3F molecule for these constants ($k_{sss'}$, $P_{ss'}$, etc.) to be available, we must estimate them. We note that the particular difference band we are interested in is the transition from $v_2(v_{s'})$ or $v_5 = 1$ to $v_3 = 2$ $(=v_s + 2)$. Hence, this theory by Yao and Overend does not apply strictly, but we may expect approximately the following:

(1) $P_s = 0$, since it is related to the intensity of an overtone transition forbidden by harmonic selection rules;

(2) $P_{ss'} = \partial^3 P/\partial Q_3^2 \partial Q_2 = 0$ since the electrical anharmonicity is small;

(3) $k_{sss'}/\omega_s \simeq 0.1$, so that $g_3 + g_4 \simeq 0.1$

Hence

$$\langle 0,1,0|P|0,0,2\rangle \simeq 0.1\ (\partial P/\partial Q_2).$$

We conclude that a first guess at the Einstein coefficients for this transition($v_3 = 2$ to $v_2 = 1$) is that they are about 1 percent of the Einstein coefficients for the fundamental ($v_2 = 1$ to 0) transition. Similarly the transition from $v_2 = 2$ to $v_5 = 1$ is about 1 percent of the value from the $v_5 = 1$ to 0 fundamental transition. The Einstein coefficient for the fundamentals can be calculated from the measured infrared intensities of the fundamental transitions, summarized for example by Russell, Needham and Overend.[52]

APPENDIX C

NUMBER	PARAMETER CHANGED	OUTPUT W/cm^2 HALF WIDTH (COLLISIONS)	COMMENTS
1	CO_2-10^3W/cm^2 4 collisions	4.1W/cm^2 90 collisions	1 collision =23 nsec. @ 10 torr
2	CO_2-10^5W/cm^2 4 collisions	4.6W/cm^2 80 collisions	
3	CO_2-10^6W/cm^2 4 collisions	4.6W/cm^2 75 collisions	
4	CO_2-10^3W/cm^2 43 collisions	16.4W/cm^2 45 collisions	shorter phase delay
5	CO_2-10^5W/cm^2 43 collisions	16.5W/cm^2 45 collisions	"
6	CO_2-10W/cm^2 CW(361 collisions)	10.9W/cm^2 90 collisions	
7	CO_2-50W/cm^2 CW(361 collisions)	15.2W/cm^2 55 collisions	shorter phase delay
8	CO_2-100W/cm^2 CW(361 collisions)	16.1W/cm^2 45 collisions	"
9	CO_2-1W/cm^2 CW(361 collisions)	no output	
10	CO_2-5W/cm^2 CW(361 collisions)	7.6W/cm^2 130 collision	longer tail
11	CO_2-10^6W/cm^2 43 collisions	16.5W/cm^2 45 collisions	
12	L=100 cm.	6.5W/cm^2 50 collisions	compaire #12-22 with #6.

NUMBER	PARAMETER CHANGED	OUTPUT	COMMENTS
13	L=300 cm.	13.4W/cm^2 110 collisions	
14	r_1=1.0 r_2=.97	12.4W/cm^2 65 collisions	
15	r_1=1.0 r_2=.99	7.6W/cm^2 125 collision	longer tail
16	CO_2-CH_3F frequency difference=0	16.8W/cm^2 65 collisions	
17	J"=12,K"=1	10.9W/cm^2 90 collisions	
18	J"=12,K"=3	16.5W/cm^2 75 collisions	different species; K'=2,K"=3
19	pressure=25 torr	28.5W/cm^2 200 collision	1 collision =9.2 nsec. @ 25 torr
20	diluent relaxation of V_{25}-V_{52} in 1600 collisions	8.1W/cm^2	CW-1W/cm^2
21	diluent relaxation of V_6 in 1600 collisions	8.0W/cm^2	CW-.52W/cm^2
22	diluent relaxation of V_{25}-V_{52} in 250 collisions	9.3W/cm^2	CW-3.8W/cm^2
23	diluent relaxation of V_{25}-V_{52} in 1600 collisions, Q-switch in 100 collisions	10.1W/cm^2	CW-3.8W/cm^2

BIBLIOGRAPHY

1. Webster New World Dictionary of the American Language, (The World Publishing Co., N.Y., 1970).

2. J.R. Meyer-Arendt, Introduction to Classical and Modern Optics, (Prentice-Hall, Inc., Englewood Cliffs, N.J., 1972).

3. Laser Focus, February, 10 (1975).

4. Laser Focus, March, 30 (1975).

5. R. Brown, Lasers, (Doubleday and Co., N.Y., 164 (1968).

6. C.N.K. Patel, W.L. Faust, and R.A. McFarlane, Bull. Amer. Phys. Soc., 9, 500 (1964).

7. P.K. Cheo in "Lasers", ed. A.K. Levine and A. J. DeMaria, Dekker, New York, 3, 111 (1971).

8. A. M. Robinson, I.E.E.E. J.O.EL. RQE 6, 560 (1970).

9. B.A. Lengyel, Lasers, (John Wiley and Sons, Inc., New York, 1971).

10. N.L. Alpert, W.E. Keiser, H.A. Szymanski, Theory and Practice of Infrared Spectroscopy, (Plenum Publishing Corp., N.Y., 1970).

11. C.N.K. Patel, Phys. Rev. Lett, 13, 617 (1964).

12. A.J. Beaulieu, Appl. Phys. Lett, 16, 504 (1970).

13. L.E. Hargrove, R.L. Fork, and M.A. Pollack, Appl. Phys. Lett, 5, 4 (1964).

14. C.A. Sacchi G. Soncini, and O. Svelto, Nuovo Cimento, 48, 58 (1967).

15. G. Goodman, J.S. Stone, and E. Thiele, J. Chem. Phy. 59, 2919 (1973).

16. G. Basov, E.P. Markin, A.N. Oraevskii, A.V. Pankrator, and A.N. Skachkov, ZhETE Pis. Red., 14, 251 (1971).

17. N.G. Basov, E.P. Markin, A.N. Oraerskii, and A.V. Pankratov, Sov. Phy. Doklady, 16, 455 (1971).

18. N.D. Artamonova, V.T. Platonenko, and R.V. Khokhlov, Soviet Physics, JETP, 31, 1185 (1970).

19. N.G. Basov, E.M. Belenov, E.P. Markin, A.N. Oraevskii, and A.V. Pankratov, Zh. EKSP. Theor. Fiz., 64, (1973).

20. G. Goodman, J.S. Stone, and E. Thiele, J. Chem. Phy., 59, 2909 (1973).

21. V.S. Letokhov, E.A. Ryabov, and O.A. Tumanov, Zh. EKSP. Theor. Fiz., 63, 2025 (1972).

22. V.S. Letokhov, A.A. Makarov, Zh. EKSP. Theor. Fiz., 63, 2064 (1972).

23. N.V. Karlov, Applied Optics, 13, 301 (1974).

24. J.P. Aldridge, R.F. Holland, H. Flicker, K.W. Nill, and T.C. Harman, J. Mol. Spectroscopy. to be published.

25. G.W. Flynn, Chemical and Biochemical Applications of Lasers, Chapter 6, Edited by C.B. Moore, (Academic Press, N.Y., 1974).

26. R.T. Bailey and F.R. Cruickshank, Molecular Spectroscopy, Chapter 4, Edited by D.A. Long, 11, (Chemical Society of London, 1974).

27. R.T. Bailey, F.R. Cruickshank, J. Farrell, D.S. Horne, A.M. North, P.B. Wilmont, and V. Tin Win, J. Chem. Phys., in press.

28. C.C. Cohen, C. Barde, and L. Henry, Compt. Rend., (1967), 265, B,; (1966), 263, B,; 619, (1966), 262.

29. R.S. McDowell, L.B. Cisprey, and R.T. Paine, J. Chem. Phys., 61, 3571 (1974).

30. T.Y. Chang, I.E.E.E. Transactions on Microwave Theory and Techniques, 22, 983 (1975).

31. T.Y. Chang and T.J. Budges, Opt. Commun., 1, 423 (1970).

32. T.Y. Chang and J.D. McGee, App. Phys. Lett., 17, 104 (1970).

33. J.I. Steinfeld, Molecules and Radiation, (Harper and Row, New York, 1974).

34. D.S. Saxon, Elementary Quantum Mechanics,(Holden-Day, 1968).

35. E. Weitz and G.W. Flynn, J. Chem. Phys., 58, 2679 (1973).

36. R.T. Bailey and F.R. Cruickshank, Chapter 4, Molecular Spectroscopy, 11, Edited by D.A. Long, (The Chemical Society, London, 1974).

37. R.N. Schwartz, Z.I. Slawsky and K.F. Herzfeld, J. Chem. Phys., 20, 1591 (1952).

38. G. Herzberg, Infrared and Raman Spectra of Polyatomic Molecules, (D. Van Nostrand Co. Inc., New York, 1945).

39. T. Oka, J. Chem. Phys., 48, 4919 (1968).

40. L. Allen and J.H. Eberly, Optical Resonance and Two Level Atoms, (Wiley-Interscience, N.Y., 1975).

41. K.P. Yates and H.H. Nielsen, Phys. Rev., 71, 349 (1974).

42. S. Reichman and J. Overend, J. Chem. Phys., 48, 3095 (1968).

43. T.S. Shimanouchi, Tables of Molecular Vibrational Frequencies, Vol. 1, (National Bureau of Standards, 1972).

44. W.L. Smith and I.M. Mills, J. Mol. Spectroscopy, 11, 11 (1963).

45. S.M. Lee and A.M. Ronn, Chem. Phys. Lett., 24, 535 (1974).

46. E. Weitz, G.W. Flynn and A.M. Ronn, J. Chem. Phys., 56, 6060 (1972).

47. E. Weitz and G.W. Flynn, J. Chem. Phys., 58, 2781 (1973).

48. F.R. Grabiner, G.W. Flynn, A.M. Ronn, J. Chem. Phys., 59, 2330 (1974).

49. S.M. Lee and A.M. Ronn, Chem. Phys. Lett., 26, 497 (1974).

50. H. Jeller, E.F. Pearson, C.L. Norris, J.C. McGurk and W.H. Flygare, J. Chem. Phys., 59, 1790 (1973).

51. K.N. Rao and A.W. Mantz, Chapter 33, Molecular Spectroscopy Modern Research, Ed. K.N. Rao and C.W. Mathews, (Academic Press, N.Y., 1972).

52. J.W. Russell, C.D. Needham and J. Overend, J. Chem. Phys., 45, 3383 (1966).

53. W.G. Wagner and B.A. Lengyel, J. Appl. Phys., 34, 2040 (1963).

54. S.M. Lee and A.M. Ronn, Chem. Phys. Lett., 26, 497 (1974).

BIOGRAPHICAL SKETCH

Harvey Charles Schau was born December 19,1949, at Kalamazoo, Michigan. In June, 1968 he was graduated from Pompano Beach High School in Pompano Beach Florida. In 1972, he received the degree of Bachelor of Science in physics, and in 1973 received the degree Master of Science in physics, both from Florida Atlantic University, in Boca Raton, Florida.

Harvey Charles Schau is married to the former Sharron Rhonda Solomon, of North Miami Florida.

I certify that I have read this study and that in my opinion it conforms to acceptable standards of scholarly presentation and is fully adequate, in scope and quality, as a dissertation for the degree of Doctor of Philosophy.

Dennis R. Keefer, Chairman
Associate Professor of Engineering Sciences

I certify that I have read this study and that in my opinion it conforms to acceptable standards of scholarly presentation and is fully adequate, in scope and quality, as a dissertation for the degree of Doctor of Philosophy.

Roland C. Anderson
Professor of Engineering Sciences

I certify that I have read this study and that in my opinion it conforms to acceptable standards of scholarly presentation and is fully adequate, in scope and quality, as a dissertation for the degree of Doctor of Philosophy.

Mark H. Clarkson
Professor of Engineering Sciences

I certify that I have read this study and that in my opinion it conforms to acceptable standards of scholarly presentation and is fully adequate, in scope and quality, as a dissertation for the degree of Doctor of Philosophy.

Willis B. Person
Professor of Chemistry

I certify that I have read this study and that in my opinion it conforms to acceptable standards of scholarly presentation and is fully adequate, in scope and quality, as a dissertation for the degree of Doctor of Philosophy.

Thomas L. Bailey
Professor of Physics

This dissertation was submitted to the Graduate Faculty of the College of Engineering and to the Graduate Council, and was accepted as partial fulfillment of the requirements for the degree of Doctor of Philosophy.
August, 1975

Dean, College of Engineering

Dean, Graduate School